

Contract No:

This document was prepared in conjunction with work accomplished under Contract No. DE-AC09-08SR22470 with the U.S. Department of Energy (DOE) Office of Environmental Management (EM).

Disclaimer:

This work was prepared under an agreement with and funded by the U.S. Government. Neither the U. S. Government or its employees, nor any of its contractors, subcontractors or their employees, makes any express or implied:

- 1) warranty or assumes any legal liability for the accuracy, completeness, or for the use or results of such use of any information, product, or process disclosed; or
- 2) representation that such use or results of such use would not infringe privately owned rights; or
- 3) endorsement or recommendation of any specifically identified commercial product, process, or service.

Any views and opinions of authors expressed in this work do not necessarily state or reflect those of the United States Government, or its contractors, or subcontractors.

We put science to work.™



**Savannah River
National Laboratory®**

OPERATED BY SAVANNAH RIVER NUCLEAR SOLUTIONS

A U.S. DEPARTMENT OF ENERGY NATIONAL LABORATORY • SAVANNAH RIVER SITE • AIKEN, SC

Dissolution Flowsheet for U-10Mo Scrap Generated from the Fabrication of High Performance Research Reactor Fuel

W. E. Daniel

T. S. Rudisill

P. E. O'Rourke

September 2019

SRNL-STI-2019-00531, Revision 0

SRNL.DOE.GOV

DISCLAIMER

This work was prepared under an agreement with and funded by the U.S. Government. Neither the U.S. Government or its employees, nor any of its contractors, subcontractors or their employees, makes any express or implied:

1. warranty or assumes any legal liability for the accuracy, completeness, or for the use or results of such use of any information, product, or process disclosed; or
2. representation that such use or results of such use would not infringe privately owned rights; or
3. endorsement or recommendation of any specifically identified commercial product, process, or service.

Any views and opinions of authors expressed in this work do not necessarily state or reflect those of the United States Government, or its contractors, or subcontractors.

Printed in the United States of America

**Prepared for
U.S. Department of Energy**

Keywords: *Dissolution, U-10Mo Alloy,
High Performance Research Reactor Fuel*

Retention: *Permanent*

Dissolution Flowsheet for U-10Mo Scrap Generated from the Fabrication of High Performance Research Reactor Fuel

W. E. Daniel
T. S. Rudisill
P. E. O'Rourke

September 2019

Prepared for the U.S. Department of Energy under
contract number DE-AC09-08SR22470.



REVIEWS AND APPROVALS

AUTHORS:

W. E. Daniel, Separations and Actinide Science Programs Date

T. S. Rudisill, Separations and Actinide Science Programs Date

P. E. O'Rourke, Analytical Development Date

TECHNICAL REVIEW:

C. A. Nash, Advanced Characterization and Processing Date

APPROVAL:

C. C. DiPrete, Separations and Actinide Science Programs, Group Leader Date

S. D. Fink, Chemical Processing Technologies Section, Director Date

K. A. Dunn, Crosscutting Pillar Program Manager Date

PREFACE OR ACKNOWLEDGEMENTS

The authors would like to acknowledge the support of the SRNL Glass Shop for not only constructing but helping to improve the design of glassware used in the dissolution experiments for the U-10Mo scrap recovery flowsheet development. The Glass Shop was able to modify equipment designs and refabricate needed glassware within a matter of days which allowed the project to proceed on schedule.

EXECUTIVE SUMMARY

The Savannah River National Laboratory was requested to develop dissolution flowsheets for low enriched uranium scrap streams generated during the fabrication of high performance research reactor (HPRR) fuel. The scrap streams include U-10Mo-Zr foil and rejected Al-clad plates. Co-rolled U-10Mo-Zr foils and Al-clad U-10Mo-Zr mini-plates which have been through the hot isostatic pressing process were obtained from BWX Technologies, Inc. for use in this work. Small-scale dissolution experiments were performed to identify the flowsheet conditions required to safely and efficiently dissolve the fuel fabrication scrap for subsequent U recovery. Experiments were performed to demonstrate the dissolution of the U-10Mo-Zr foil, removal of the Al cladding from the mini-plates, and the dissolution of the mini-plates following cladding removal.

A series of solubility experiments was performed to find an optimum nitric acid concentration for the U-10Mo-Zr foil dissolution where no precipitates would form. The dissolution of small pieces of the foil at 20 g/L U with 0.05 M fluoride and 50 g/L U with 0.1 M fluoride and 0.5 M $\text{Fe}(\text{NO}_3)_3$ using 4 and 5 M HNO_3 did not show any evidence of precipitates. The fluoride was added to insure there would be no exothermic dissolution of a potential UZr_2 intermetallic compound. The Fe was added to prevent the precipitation of uranyl molybdate at the higher U concentration. However, a foil dissolution experiment at 20 g/L U using 3 M HNO_3 and 0.05 M fluoride formed a reddish precipitate that was easily re-suspended and eventually re-dissolved. The dissolution of a piece of foil at 50 g/L U with 0.1 M fluoride and 0.5 M $\text{Fe}(\text{NO}_3)_3$ using 3 M HNO_3 formed a white precipitate that was identified as a Zr-Mo compound ($\text{ZrMo}_2\text{O}_5(\text{OH})_2(\text{H}_2\text{O})_2$). There were no U products identified in the precipitate. Based on these results, the use of a sufficient volume of 4 M HNO_3 to maintain the final acid concentration greater than approximately 3.5 M is recommended to dissolve scrap U-10Mo-Zr foil at the boiling point of the solution when targeting 20 or 50 g/L U. The fluoride concentration should be adjusted to establish a 4:1 mole ratio of fluoride to Zr and 0.5 M $\text{Fe}(\text{NO}_3)_3$ added to the solution when targeting a final U concentration of 50 g/L.

To estimate the processing time for dissolving the U-10Mo-Zr foil, dissolution rate experiments were performed. The dissolution rates of the U-10Mo-Zr foil in 4 M HNO_3 for both 20 g/L U (0.05 M fluoride) and 50 g/L U (0.1 M fluoride and 0.5 M $\text{Fe}(\text{NO}_3)_3$) flowsheets were measured at the boiling point of the solutions. The dissolution rates were in the range of $1.2\text{E-}02$ to $1.5\text{E-}02$ $\text{g}/\text{cm}^2/\text{min}$ for both flowsheets which were similar to rates measured during prior LEU dissolution experiments. In each dissolution experiment, there was an initial slower dissolution rate of $4\text{E-}03$ to $6\text{E-}03$ $\text{g}/\text{cm}^2/\text{min}$ which was attributed to the dissolution of the Zr diffusion barrier on the exterior of the U-10Mo foil.

To provide offgas characterization data for potential flammability concerns, the H_2 generation rates during the dissolution of U-10Mo-Zr foil at 20 g/L U (0.05 M fluoride) and 50 g/L (0.1 M fluoride and 0.5 M Fe) were measured using Raman spectroscopy. The peak H_2 generation rates were 0.02 $\text{cm}^3/\text{min}/\text{cm}^2$ and 0.09 $\text{cm}^3/\text{min}/\text{cm}^2$, respectively. The H_2 generation rates increased once the boiling point of the solution was reached. Since the acid concentrations were the same in both experiments, the higher H_2 generation rate for the 50 g/L U dissolution was attributed to the higher fluoride concentration (about twice that of the 20 g/L U dissolution). The H_2 generation rates are small compared to the H_2 generation rate during Hg-catalyzed dissolution of Al alloys (e.g., Al-1100) in HNO_3 which normally peak around 2 $\text{cm}^3/\text{min}/\text{cm}^2$. The small amount of H_2 generated during the dissolution of U-10Mo-Zr foil would be easily managed by supplying an air purge to the dissolver to dilute the concentration if necessary.

The use of a caustic solution was selected to remove the Al cladding from failed HPRR fuel plates prior to dissolving the U-10Mo-Zr foil to reduce the amount of fluoride in down-stream processes which will reduce the potential for corrosion of equipment and precipitation of fluoride-containing solids. For the Al decladding phase, parameters were initially selected based on the caustic dissolution flowsheet

demonstrated at the Savannah River Site F-Canyon facility to remove Al-6063 cladding from natural and depleted U targets used for Pu production. However, the F-Canyon decladding flowsheet was not successful for removing the Al-6061 cladding from the U-10Mo-Zr mini-plates. The NaOH concentration was not sufficient to prevent precipitation of aluminum hydroxide-containing compounds which terminated the Al dissolution. Small scale decladding experiments subsequently demonstrated that a solution containing 9.37 moles of NaOH and 1.27 moles of NaNO₃ per mole of Al was sufficient to declad the mini-plates and prevent the precipitation of Al as sodium aluminate and other compounds. The H₂ offgas generation rate during mini-plate decladding produced a peak rate of about 2 cm³/min/cm² or a rate comparable to the Hg-catalyzed dissolution of Al-1100 in HNO₃. The H₂ offgas generation rate would be manageable with an appropriately sized air purge to the dissolver to dilute the H₂ concentration.

The dissolution of a piece of a U-10Mo-Zr mini-plate following cladding removal was demonstrated using the flowsheet developed for unclad foil. Dissolution of the declad foil at 20 g/L U (0.05 M fluoride) in 4 M HNO₃ resulted in no post-dissolution precipitation. The total offgas generation per unit surface area was similar to the unclad U-10Mo-Zr foil. During both dissolutions, the primary off gases were NO and NO₂ (approximately 90-99% of total offgas) with the balance being H₂. The H₂ generation rate for the declad foil was noticeably lower than the unclad foil. This is likely due to the formation of oxide on the surface of the declad foil as opposed to the pristine condition of the unclad foil.

TABLE OF CONTENTS

LIST OF TABLES	ix
LIST OF FIGURES	ix
LIST OF ABBREVIATIONS.....	xii
1.0 Introduction.....	1
1.1 Background	1
1.2 Dissolution of U-10Mo Alloys.....	3
1.3 U-Zr Intermetallic Compounds	5
1.4 Caustic Dissolution of U Metal	6
1.5 Objectives.....	7
2.0 Experimental Procedure.....	7
2.1 USHPRR Fuel Fabrication Scrap	7
2.2 U-10Mo-Zr Foil.....	8
2.3 Al-clad U-10Mo-Zr Mini-plates.....	9
2.3.1 Al Cladding Removal	10
2.3.2 Dissolution U-10Mo-Zr Foil Following Cladding Removal	10
2.4 Dissolving System.....	10
2.4.1 Raman Spectrometer.....	11
2.4.2 Raman Spectrometer Calibration and Sampling Method	12
2.5 Quality Assurance	13
3.0 Results and Discussion	13
3.1 U-10Mo-Zr Foil.....	13
3.1.1 Effect of HNO ₃ on Foil Dissolution	13
3.1.2 Dissolution Rate of Foil.....	16
3.1.3 Characterization of Offgas During Foil Dissolution.....	19
3.2 U-10Mo-Zr Mini-plate	22
3.2.1 Al Cladding Dissolution	22
3.2.2 Flowsheet Demonstration for Declad Mini-plate	33
4.0 Conclusions.....	36
5.0 Future Work	37
6.0 References.....	38

LIST OF TABLES

Table 1-1. Definition of Scrap Streams	2
Table 2-1. Summary of Experimental Conditions Used for U-10Mo-Zr Foil Dissolutions	8
Table 2-2. U-10Mo-Zr Coupon Characteristics.....	9
Table 2-3. U-10Mo-Zr Mini-plate Characteristics.....	9
Table 2-4. Masses and Dimensions of Cut U-10Mo-Zr Mini-plates	9
Table 2-5. Calibration Gases for MS and Raman Analyzers	12
Table 2-6. Standard Deviation of Raman Concentrations with Respect to Calibrated Values	13
Table 3-1. Boiling Points for Dissolved Foil Solubility Experiments	14
Table 3-2. Composition of Dissolving Solutions from Foil Solubility Experiments.....	16
Table 3-3. Experiment 159 – Dissolution Data for U-10Mo-Zr foil at 20 g/L U	16
Table 3-4. Experiment 164 – Dissolution Data for U-10Mo-Zr foil at 50 g/L U	18
Table 4-1. Summary of Results for Dissolution of U-10Mo-Zr Foil.....	36
Table 4-2. Summary of Results for Al Decladding of U-10Mo-Zr Mini-plates	36

LIST OF FIGURES

Figure 1-1. Schematic Diagram of a Typical U-10Mo Fuel Plate (not to scale-units in millimeters).....	1
Figure 1-2. Scrap Streams from USHPRR Fuel Fabrication and Planned Disposition	2
Figure 1-3. Solubility of Mo in HNO ₃ Solutions Containing U.....	3
Figure 1-4. Solubility of Mo in HNO ₃ Solutions Containing U and 0.5 M Fe(NO ₃) ₃	4
Figure 1-5. Solubility of Mo in HNO ₃ Solutions Containing U and 0 and 0.5 M Fe(NO ₃) ₃	4
Figure 1-6. Solubility of Mo in 1 M HNO ₃ Containing Other Metal Nitrates	5
Figure 1-7. U-Zr Phase Diagram.....	6
Figure 2-1. U-10Mo-Zr Foil and Al-clad Mini-plates	8
Figure 2-2. Dissolver Setup with Online Raman Offgas Analyzer.....	10
Figure 2-3. Alternate Dissolver Apparatus (left 150-mL Vessel and right 600-mL Vessel)	11
Figure 3-1. Exp 156 Solution After 1 day Settling (left) Before Mixing and (right) After Mixing.....	14
Figure 3-2. Exp 156 Solution After 12 days Settling (left) and 21 days Settling (right)	14

Figure 3-3. Exp 161 Solution After Cooling – White Solids on Glassware 15

Figure 3-4. XRD of Exp 161 Precipitate – 50 g/L U, 3 M HNO₃, 0.1 M Fluoride, and 0.5 M Fe..... 15

Figure 3-5. Experiment 159 – Dissolution Rates for U-10Mo-Zr foil at 20 g/L U..... 17

Figure 3-6. Experiment 164 – Dissolution Rates for U-10Mo-Zr foil at 50 g/L U..... 18

Figure 3-7. Experiment 164 – Progressive Removal of Zr Diffusion Barrier..... 19

Figure 3-8. Exp 160 Offgas Generation Rates from the Dissolution of U-10Mo-Zr Foil in 4 M HNO₃ and 0.05 M Fluoride to a Final U concentration of 20 g/L..... 20

Figure 3-9. Exp 165 Offgas Generation Rates from the Dissolution of U-10Mo-Zr Foil in 4 M HNO₃ and 0.1 M Fluoride to a Final U concentration of 50 g/L..... 21

Figure 3-10. H₂ Generation Rates from the Dissolution of U-10Mo-Zr Foil..... 22

Figure 3-11. Exp 166 Offgas Generation Rates from the Caustic Partial Decladding of Piece 1 of Mini-plate A2C117 in 0.44 M NaOH and 0.33 M NaNO₃ 23

Figure 3-12. Exp 166 H₂ Generation Rate from the Caustic Partial Decladding of Piece 1 of Mini-plate A2C117 in 0.44 M NaOH and 0.33 M NaNO₃..... 23

Figure 3-13. Caustic Decladding of Piece 1 of Mini-plate A2C117 after 101 min of Boiling 24

Figure 3-14. White Solids from the Caustic Decladding of Piece 1 of Mini-plate A2C117..... 24

Figure 3-15. Near the Start of Boiling during Decladding of Piece 1 of Mini-plate A2C117 in 0.44 M NaOH (left) and 2 M NaOH (right) 25

Figure 3-16. 20 min After the Start of Boiling during Decladding of Piece 1 of Mini-plate A2C117 in 2 M NaOH..... 25

Figure 3-17. Declad Piece 1 of Mini-plate A2C117 26

Figure 3-18. Exp 168 Offgas Generation Rates from the Partial Decladding of Piece 3 of Mini-plate A2C116 using a 1 M Solution of NaOH Containing 1.5 M NaNO₃..... 27

Figure 3-19. H₂ Generation Rate from the Decladding of Piece 3 of Mini-plate A2C116 using a 1 M Solution of NaOH Containing 1.5 M NaNO₃ 27

Figure 3-20. Decladding of Piece 3 of Mini-plate A2C116 Following 30 min of Boiling in 1 M NaOH. 28

Figure 3-21. Exp 168A Offgas Generation Rates from Partial Decladding of Piece 3 of Mini-plate A2C116 using 2 M NaOH and 1.5 M NaNO₃..... 29

Figure 3-22. Exp 168A H₂ Generation Rate from Partial Decladding of Piece 3 of Mini-plate A2C116 using 2 M NaOH and 1.5 M NaNO₃ 29

Figure 3-23. 13 min (left) and 29 min (right) into Boiling during the Decladding of Piece 3 of Mini-plate A2C116 using 2 M NaOH 30

Figure 3-24. XRD of Experiment 166 Precipitate – 20 g/L U, 0.44 M NaOH, and 0.33 M NaNO₃ 31

Figure 3-25. Exp 168B Offgas Generation Rates from the Decladding of Piece 3 of Mini-plate A2C116 using 2.6 M NaOH and 0.33 M NaNO ₃	32
Figure 3-26. Exp 168B H ₂ Generation Rate from the Decladding of Piece 3 of Mini-plate A2C116 using 2.6 M NaOH and 0.33 M NaNO ₃	32
Figure 3-27. 2 min (left) and 27 min (right) into Boiling during the Decladding of Piece 3 of Mini-plate A2C116 using 2.6 M NaOH	33
Figure 3-28. Full Declad Piece 3 of Mini-plate A2C116.....	33
Figure 3-29. Exp 169 Offgas Generation Rates from the Dissolution of U-10Mo-Zr Foil from the Decladding of Piece 3 of Mini-plate A2C116 Targeting 20 g/L U in 4 M HNO ₃ and 0.05 M Fluoride	34
Figure 3-30. H ₂ Generation Rate from the Dissolution of U-10Mo-Zr Foil from the Decladding of Piece 3 of Mini-plate A2C116 Targeting 20 g/L U in 4 M HNO ₃ and 0.05M Fluoride	35
Figure 3-31. Comparison of the Total Offgas Generation Rates from the Dissolution of the Declad U-10Mo-Zr Foil in Exp 169 and the Unclad Foil Dissolved in Exp 160.....	35

LIST OF ABBREVIATIONS

ANL	Argonne National Laboratory
ATR	Advanced Test Reactor
BWXT	BWX Technologies, Inc.
HEU	highly enriched U
HFIR	High Flux Isotope Reactor
HIP	hot isostatic pressing
ICPMS	inductively-coupled mass spectrometry
LEU	low enriched U
M ³	Material Management and Minimization
MIT	Massachusetts Institute of Technology
MURR	University of Missouri Research Reactor
NBSR	National Bureau of Standards Reactor
NNSA	National Nuclear Security Administration
SRNL	Savannah River National Laboratory
SRS	Savannah River Site
USHPRR	United States High Performance Research Reactor
XRD	x-ray diffraction
Y-12	Y-12 National Security Complex

1.0 Introduction

1.1 Background

The National Nuclear Security Administration (NNSA) Office of Material Management and Minimization (M³) United States High Performance Research Reactor (USHPRR) project is developing a low enriched U-10Mo fuel as a candidate replacement for the highly enriched U (HEU) fuels currently being used in the U.S. high performance reactors. The USHPRR's include the Massachusetts Institute of Technology (MIT) Reactor, University of Missouri Research Reactor (MURR), National Bureau of Standards Reactor (NBSR) at the National Institute of Standards and Technology, Advanced Test Reactor (ATR) at the Idaho National Laboratory, and High Flux Isotope Reactor (HFIR) at Oak Ridge National Laboratory. The proposed baseline fuel utilizes an Al cladding similar to the present generation of fuel; however, the fissionable component of the fuel consists of a low enriched U-10Mo monolithic alloy with a thin layer of Zr separating the fuel core from the cladding. The USHPRR Project team is working with the national laboratory complex to develop and qualify the low enriched U (LEU) fuel and facilitate the research reactor conversions starting with the Nuclear Regulatory Commission licensed HPRR's, (i.e., MIT, MURR and NBSR reactors).¹

The U-10Mo fuel design is based on a monolithic U-10Mo alloy, enclosed in Al cladding (alloy Al-6061), with a diffusion/bonding interlayer composed of Zr. A schematic diagram of a foil-type element under consideration is shown in Figure 1-1 (units are in millimeters). The new LEU fuel design provides a U density much greater than in conventional HEU dispersion fuel designs, which is required to convert the USHPRR's to LEU fuels.¹

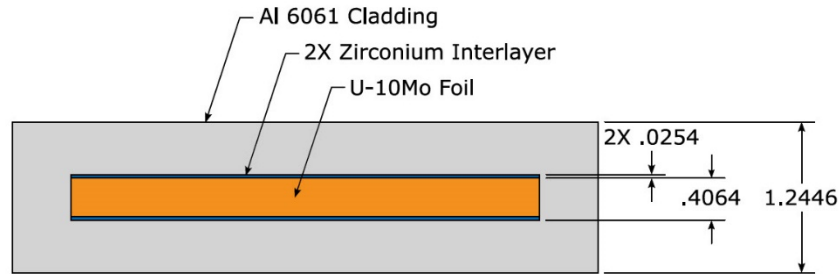


Figure 1-1. Schematic Diagram of a Typical U-10Mo Fuel Plate (not to scale-units in millimeters)

The casting operations used to produce the U-10Mo alloy and the fuel fabrication processes result in the generation of scrap streams containing LEU which must be recovered. Figure 1-2 provides a list of the scrap streams generated in both casting and fuel fabrication and their disposition paths. The scrap streams are defined in Table 1-1.¹ The aqueous recovery processes proposed by Dunn et al. for the U-Mo scrap streams are based on the dissolution of the materials using HNO₃-based flowsheets. The Al cladding on plates that do not meet specification after the hot isostatic pressing (HIP) operation may be initially removed using a caustic solution (e.g., NaOH). Other materials such as fluoride or Fe(III) may be added to the dissolving solution to increase the solubility of other components of the fuel (e.g., Zr and Mo).¹

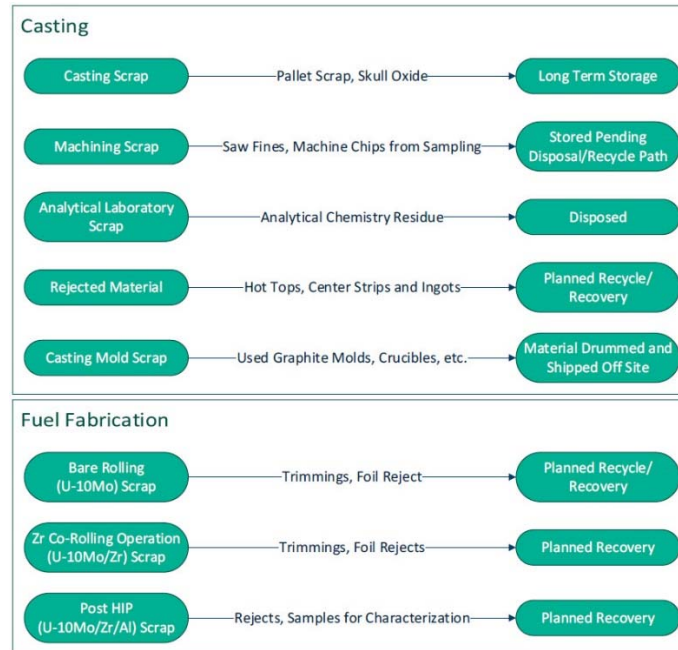


Figure 1-2. Scrap Streams from USHPRR Fuel Fabrication and Planned Disposition

Table 1-1. Definition of Scrap Streams

Scrap Stream	Definition
Analytical Chemistry Residue	Liquid residues remaining after the analytical chemistry analyses are completed
Rejected Center Strip	Strip of material between the two ingots that is drilled to supply material for chemical analysis
Crucible	Graphite vessel in which the materials are melted for casting
Trimmings	Portion of co-rolled plates that are removed due to imperfections
Reject Foils	Foils that do not meet specification and cannot be accepted with a non-conformance report
Hot Tops	Top portion of the casted plate that is removed after casting
Ingots	Portion of the casted plate that is removed for further processing (rolling, etc.)
Machine Chips from Sampling	Machining fines remaining after samples of the center strip are removed with a drill for chemical analysis
Pallet Scrap	Material that leaks out or spills out of mold during a pour (which is heavily oxidized and carbon-contaminated with non-U elements)
Graphite Molds	Graphite material such as mold housing, plates, etc. used in the casting process
Rejects (Post HIP)	Plates that do not meet specification after the HIP operation (Zr coated foils encased in Al)
Characterization Samples	Portions of center strip that are removed with a drill for analytical chemistry
Saw Fines	Material that remains after the sawing/machining operations
Skull	Material that remains in the crucible after the molten material is poured into the mold housing
Trimming	Pieces of foils that are removed after bare rolling or co-rolling

1.2 Dissolution of U-10Mo Alloys

Dissolution flowsheets have been demonstrated for both U-Mo reactor fuels and the scrap generated from the fabrication of fuel from U-Mo alloys. Stepinski et al. summarized previous work used to develop dissolution flowsheets for irradiated U-Mo fuels as part of the NNSA's Fuel Fabrication Capability Project in 2008.² The document provides a comprehensive review of U-Mo dissolution technology up to this date. Stepinski et al. and Jerden et al. used this information as the basis for flowsheet recommendations for the dissolution of U-Mo scrap generated during the fabrication of USHPRR fuels.^{3,4} Researchers at Argonne National Laboratory (ANL) performed small-scale dissolutions using 0.2 to 1.2 g of U-10Mo, U-8Mo-Zr, and U-10Mo-Zr foils to demonstrate flowsheets for the dissolution of HPPR fuel fabrication scrap.⁵⁻⁷ The dissolution of off-specification fuel plates was simulated by dissolving small pieces of an Al-6061 alloy prior to the U-Mo-Zr foil. One issue that was not completely resolved in these studies was the precipitation of orange-red solids in solutions containing nominally 20 g/L U. The solids subsequently dissolved, but their origin and disappearance were not completely understood.

The most important consideration in designing a U-Mo dissolution process is the limited solubility of Mo in $\text{UO}_2(\text{NO}_3)_2$ solutions. An extensive study on the solubility of Mo in nitrate-based media in the presence of $\text{Fe}(\text{NO}_3)_3$ and other metal salts was performed by Faugeras.⁸ The solubility of Mo as a function of the U and HNO_3 concentrations is shown in Figure 1-3.

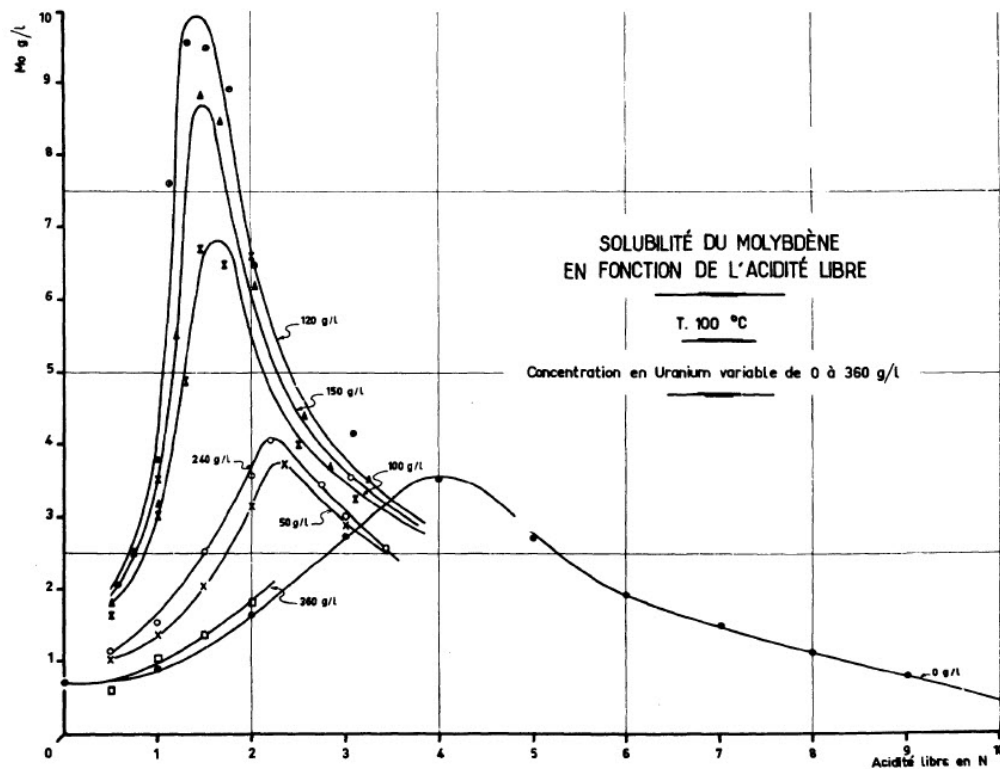


Figure 1-3. Solubility of Mo in HNO_3 Solutions Containing U

Faugeras et al. also completed extensive studies on the solubility of Mo in $\text{UO}_2(\text{NO}_3)_2 - \text{HNO}_3$ solutions in the presence of 0.25-1.5 M $\text{Fe}(\text{NO}_3)_3$. Data from this study for solutions containing 0.5 M $\text{Fe}(\text{NO}_3)_3$ are plotted in Figure 1-4.⁸ The increased solubility of Mo can be attributed to the formation of a negatively charged Fe-Mo complex which prevents precipitation of uranyl molybdate.⁹ Based on the increased solubility of Mo in HNO_3 solutions containing U and Fe, one strategy for dissolving U-10Mo scrap to higher terminal U concentrations and lower terminal HNO_3 concentrations is the addition of $\text{Fe}(\text{NO}_3)_3$ to

the dissolving solution. However, this dissolution strategy must be balanced against increasing nuclear safety concerns with increasing ^{235}U concentrations and the generation of more waste from the addition of Fe. The Mo solubility data from Faugas et al.⁸ for 0 and 0.5 M Fe for various U g/L concentrations at 100 °C was combined in Figure 1-5 to show how the HNO_3 and Fe molarity impacts Mo solubility.

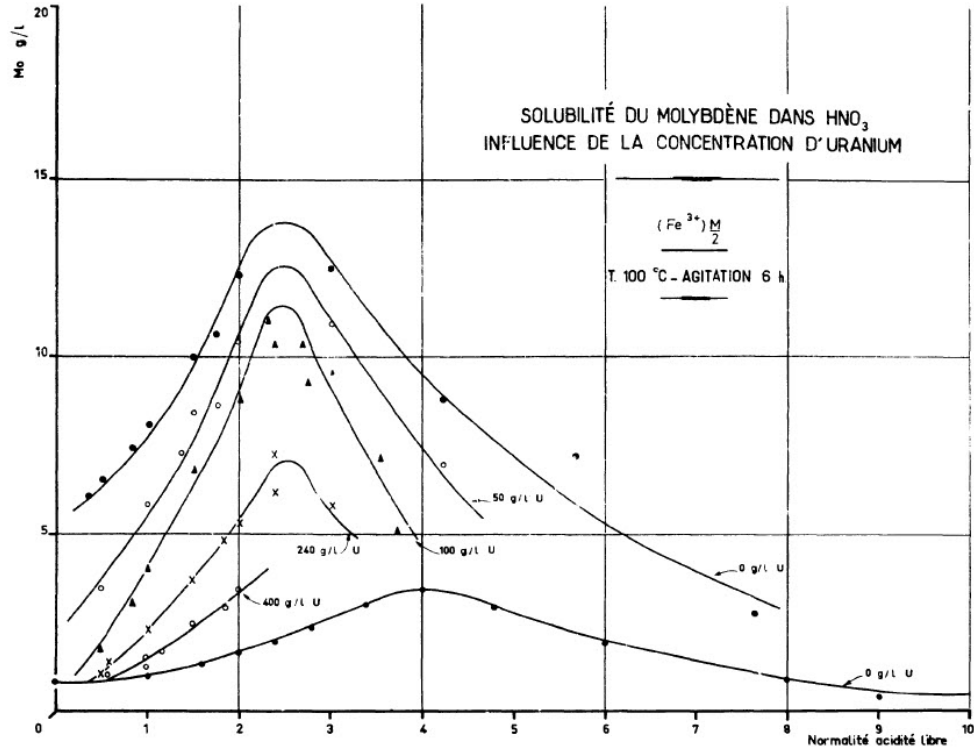


Figure 1-4. Solubility of Mo in HNO_3 Solutions Containing U and 0.5 M $\text{Fe}(\text{NO}_3)_3$

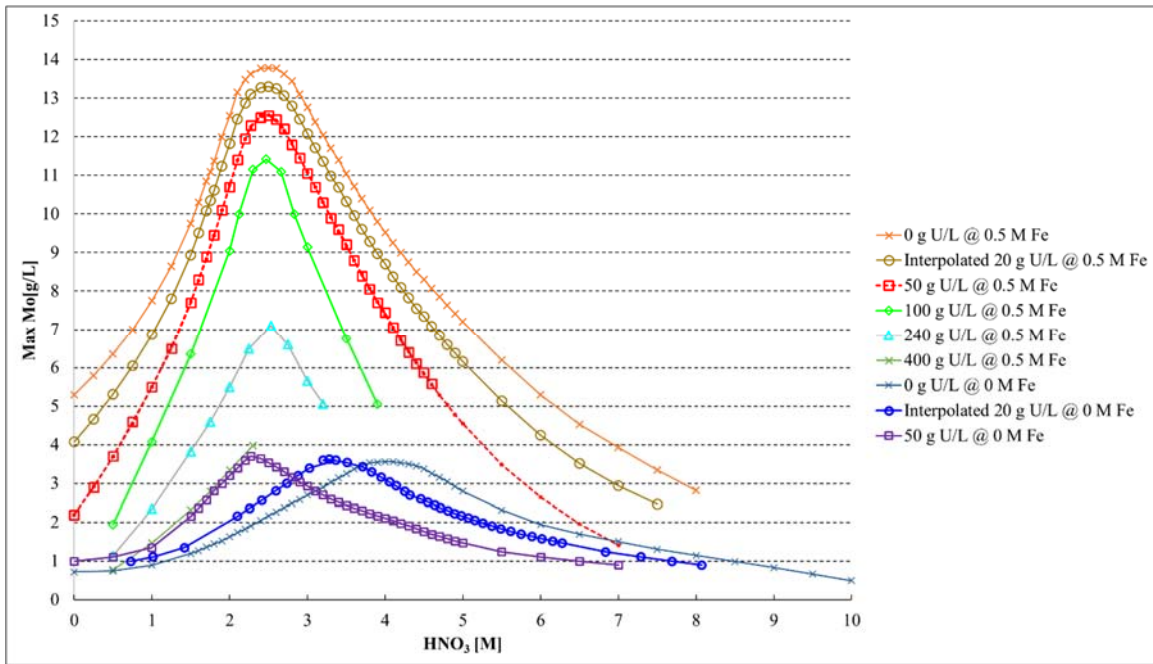


Figure 1-5. Solubility of Mo in HNO_3 Solutions Containing U and 0 and 0.5 M $\text{Fe}(\text{NO}_3)_3$

The presence of other nitrate salts such as $\text{Al}(\text{NO}_3)_3$ also has a significant effect on the solubility of Mo in HNO_3 solutions. Figure 1-6 shows data measured by Faugas et al. for Mo solubility in 1 M HNO_3 as a function of the total nitrate concentration.⁸ Separate curves for $\text{Fe}(\text{NO}_3)_3$, $\text{UO}_2(\text{NO}_3)_2$, and $\text{Al}(\text{NO}_3)_3$ are provided. The presence of Al in the cladding of a U-10Mo-Zr fuel plate is an important concern if a catalyst such as fluoride is used to simultaneously dissolve all components of the plate. The effect of the U, Al, and Zr concentrations on the solubility of Mo must be addressed. One option for eliminating the effect of Al on the solubility of Mo is to remove the Al cladding prior to the dissolution of the U-10Mo-Zr foil. The Al cladding can be dissolved using a caustic solution (e.g., NaOH) without dissolving the U-10Mo-Zr foil. Usually NaNO_3 is added to the solution to suppress the evolution of H_2 during dissolution.¹⁰

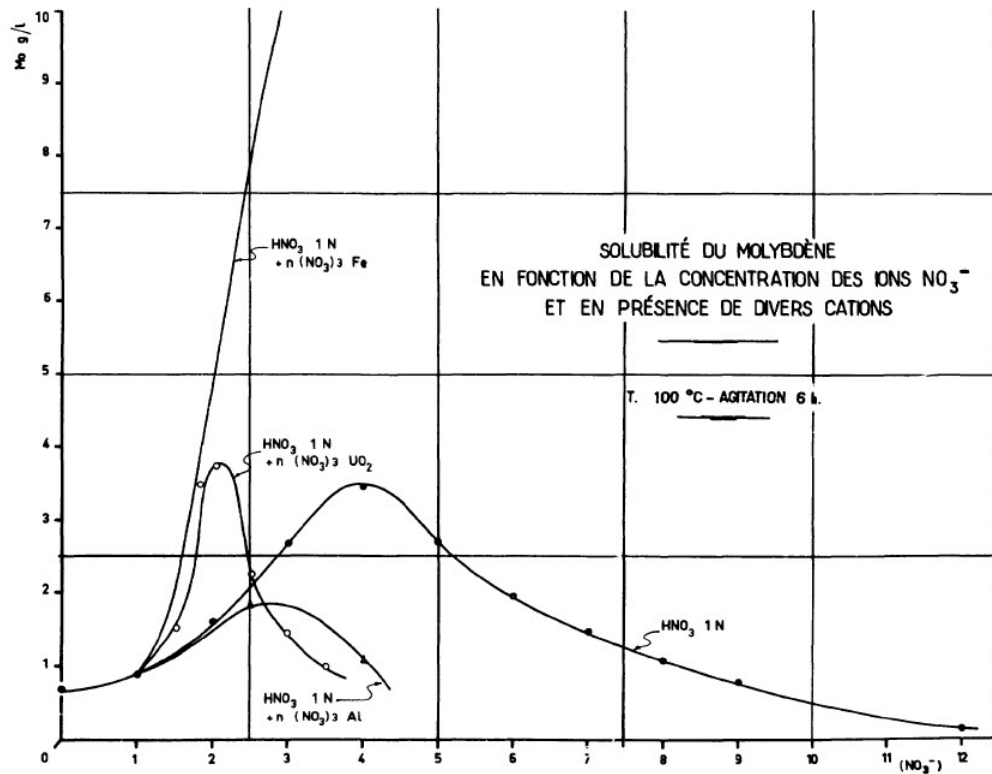


Figure 1-6. Solubility of Mo in 1 M HNO_3 Containing Other Metal Nitrates

1.3 U-Zr Intermetallic Compounds

When dissolving the U-10Mo-Zr foils and plates, one potential area of concern is the presence of U-Zr intermetallic compounds at the interface between the U and Zr. Explosions, fires, vigorous to violent reactions, and other off-normal events involving the dissolution of U-Zr alloys in HNO_3 have been documented within the Department of Energy complex dating back to the 1950's.¹¹ The exothermic reactions result from the rapid oxidation of finely divided solids released by the preferential dissolution of the U metal matrix. The explosive portion of such solids has been identified as an intermetallic compound with the approximate composition of UZr_2 .¹² Other researchers have cited UZr_3 as the stoichiometry and refer to the intermetallic compound as the epsilon phase in the U-Zr phase diagram; although, more recent work refers to UZr_2 as the delta phase. Larsen et al. concluded that depending on the composition, homogeneity, and previous thermal history, U-Zr alloys with 1 to 50 wt % Zr will contain some amount of the finely divided delta phase in a matrix of alpha-U. Concentrations below 1 wt % were not reported to exhibit exothermic behavior.¹³

The extent of the formation of the UZr_2 phase at the diffusion barrier interface with the fuel during fuel fabrication is not known; however, there is sufficient Zr and the necessary heating to promote its formation. The prototypical U-10Mo-Zr foil for the fuel plate shown in Figure 1-1 contains between 4 and 5 wt % Zr. The phase diagram for the U-Zr system shown in Figure 1-7 indicates that the UZr_2 phase will form when temperatures are high enough to promote diffusion yet lower than approximately 600 °C.¹⁴ These conditions are present during hot rolling and HIP operations used during USHPRR fuel fabrication.⁴ Therefore, the dissolution flowsheet for the U-10Mo-Zr foil must be developed assuming that the UZr_2 phase is present in scrap foil and rejected fuel plates.

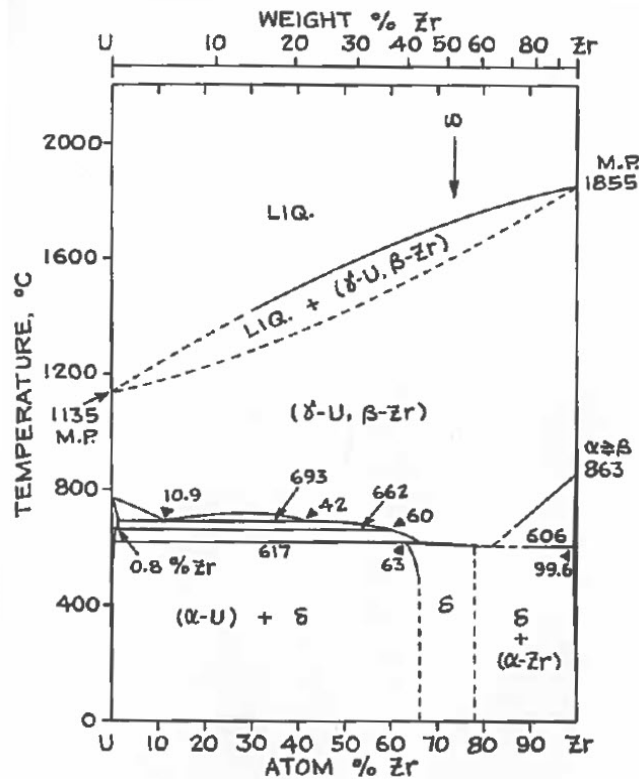


Figure 1-7. U-Zr Phase Diagram

(The UZr_2 phase is designated as the delta (δ) phase in the diagram.)

For Zr concentrations above 1 wt %, the addition of fluoride in sufficient quantities will eliminate the explosion hazard. The HNO_3 – fluoride solution dissolves the U-Zr intermetallic phase as rapidly as it is exposed by the dissolution of the U matrix. In the absence of other complexing species, Larsen et al. demonstrated that a 4 to 1 mole ratio of fluoride to Zr was the minimum required to prevent the formation of finely divided UZr_2 solids. Throughout the dissolutions performed in this medium, the alloys remained shiny and no trace of the explosive solids were detected.¹³ The addition of fluoride inhibits the instantaneous oxidation of the UZr_2 phase by catalyzing its dissolution through complexation. The formation of stable Zr fluoride complexes ($ZrF_{4(aq)}$, ZrF_3^+ , ZrF_2^{2+} and ZrF^{3+}) allows the UZr_2 intermetallic phase to dissolve at a rate similar to the U metal and prevents the buildup of potentially explosive material.⁴

1.4 Caustic Dissolution of U Metal

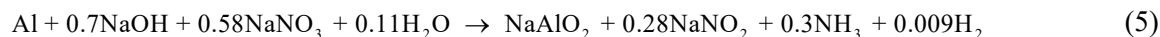
Prior to designing the dissolution flowsheet for rejected U-10Mo-Zr fuel plates, the strategy for removing the Al cladding must be selected. Two options exist for the dissolution of the cladding material. The entire fuel plate can be dissolved in a mixture of nitric and hydrofluoric acids with sufficient acid and fluoride to

dissolve the Al cladding, the Zr-bonding layer, and the U-10Mo alloy. Alternatively, the Al cladding can first be removed using a NaOH solution to dissolve the Al with little to no effect on the U-10Mo-Zr foil. The removal of the Al cladding prior to the dissolution of the foil will reduce the amount of fluoride handled in down-stream processes which will reduce the potential for corrosion of equipment and precipitation of fluoride-containing solids. If required, a flowsheet can be developed later in which the entire plate is dissolved in a HNO₃ solution containing fluoride. The use of a Hg catalyst to facilitate the dissolution of the Al cladding was not considered a viable processing option due to the creation of a mixed low level waste.

Caustic Al dissolution is performed using a NaOH solution containing NaNO₃. The nitrate is used to suppress the evolution of H₂ by altering the reaction mechanism so that mostly NH₃ is produced. The reactions (1-4) thought to be involved during the dissolution processes are shown below.



Equation (5), derived empirically from laboratory-scale studies based on conditions used at the Savannah River Site's (SRS's) F-Canyon facility to remove Al cladding from natural and depleted U targets best represents the total reaction.¹⁰



For the flowsheet development, a two-step dissolution process was demonstrated in which the Al cladding is removed using a caustic solution. The Al-containing solution will be transferred from the dissolver and discarded as waste prior to the dissolution of the U-10Mo-Zr foil in an acidic solution.

1.5 Objectives

The Savannah River National Laboratory (SRNL) was requested to develop dissolution flowsheets for four categories of scrap representative of the streams shown in Figure 1-2 which will be processed for U recovery.^{15,16} The casting scraps include both U-10Mo metal and oxide. Co-rolled U-10Mo-Zr foils and Al-clad U-10Mo-Zr mini-plates which have been through the HIP process were shipped to SRNL from BWX Technologies, Inc. (BWXT). The materials from BWXT are representative of the scrap streams generated during fuel fabrication. Skull oxide and metal samples from the Y-12 National Security Complex (Y-12) casting process will be shipped to SRNL at a later date. The SRNL will use these materials in experiments to develop and demonstrate flowsheets which can be used to safely and efficiently dissolve the fabrication and casting scraps for subsequent U recovery. The U-Mo dissolution process(es) will be designed to accommodate downstream processing without significant solution adjustments to the extent possible. Following dissolution, the U will be purified and recovered as a UO₂(NO₃)₂ solution using a modified PUREX process.

2.0 Experimental Procedure

2.1 USHPRR Fuel Fabrication Scrap

Co-rolled U-10Mo-Zr foil and Al-clad U-10Mo-Zr mini-plates were shipped to SRNL from BWXT for use in dissolution experiments as representative materials for scrap generated during the fabrication of USHPRR fuel. The foil and mini-plates were used in laboratory-scale experiments to demonstrate optimized dissolution flowsheets. The flowsheets were designed to ensure that solids are not generated

during the dissolution and that the solution is stable from precipitation once the dissolution is complete. Photographs of the foil and mini-plates are shown in Figure 2-1.



Foil



Mini-plates

Figure 2-1. U-10Mo-Zr Foil and Al-clad Mini-plates

2.2 U-10Mo-Zr Foil

Experiments were performed with the U-10Mo-Zr foil to evaluate its dissolution at terminal U concentrations of 20 and 50 g/L using HNO₃ concentrations ranging from 3 to 5 M. In the experiments performed at 50 g/L U, 0.5 M Fe(NO₃)₃ was added to the dissolving solution to prevent the precipitation of uranyl molybdate based on Mo solubility data examined. The predicted and maximum Mo solubility values from Faugeras et al.⁸ for the selected U and HNO₃ concentrations are shown in Table 2-1. A small amount of fluoride (as KF) was also added to the solutions targeting a 4 to 1 mole ratio of fluoride to Zr to prevent the formation of finely divided UZr₂ solids which have the potential to explosively dissolve in HNO₃ solution if sufficient fluoride is not present to catalyze the Zr dissolution. All experiments were performed at the boiling point of the solution. A summary of the conditions which were used for each experiment are provided in Table 2-1. The HNO₃ concentration for experiments 159-160 and 164-165 was selected based on the results from Experiments 156-158 and 161-163, respectively.

Table 2-1. Summary of Experimental Conditions Used for U-10Mo-Zr Foil Dissolutions

Exp. No.	Final U (g/L)	Objective (Evaluate)	Initial HNO ₃ (M)	Fluoride (M)	Fe(NO ₃) ₃ (M)	Volume (L)	Pred Mo (g/L)	Max Mo (g/L)
156	20	U-Mo Solubility	3.00	0.05	0	0.315	2.2	2.8
157	20	U-Mo Solubility	4.00	0.05	0	0.296	2.2	3.5
158	20	U-Mo Solubility	5.00	0.05	0	0.299	2.2	2.5
159	20	Dissolution Rate	4.00	0.05	0	0.342	2.2	3.5
160	20	Offgas Generation	4.00	0.05	0	0.301	2.2	3.5
161	50	U-Mo Solubility	3.00	0.1	0.50	0.127	5.6	10.5
162	50	U-Mo Solubility	4.00	0.1	0.50	0.133	5.6	11.2
163	50	U-Mo Solubility	5.00	0.1	0.50	0.134	5.6	7.4
164	50	Dissolution Rate	4.00	0.1	0.50	0.131	5.56	11.2
165	50	Offgas Generation	4.00	0.1	0.50	0.121	5.56	11.2

The U-10Mo-Zr foil was cut using tin snips into nominally 1-in x 1-in coupons for use in dissolution experiments. The mass of the coupons ranged between approximately 7 and 8 grams. The surface area (SA)

of a coupon was calculated using equation (1) where L is the length, W is the width, and T is the thickness of the coupon. The masses, dimensions, and surface areas of the coupons used in the experiments are provided in Table 2-2.

$$SA = 2(L \times W + L \times T + W \times T) \quad (1)$$

Table 2-2. U-10Mo-Zr Coupon Characteristics

Exp. No.	Mass (g)	Length (cm)	Width (cm)	Thickness (cm)	Surface Area (cm²)
156	7.2677	2.652	2.469	0.069	13.80
157	6.8344	2.594	2.331	0.072	12.80
158	6.9082	2.486	2.485	0.070	13.05
159	7.9051	3.093	2.264	0.069	14.74
160	6.9573	2.467	2.572	0.070	13.39
161	7.3406	2.442	2.687	0.069	13.83
162	7.6671	2.798	2.606	0.067	15.31
163	7.7216	2.425	2.915	0.070	14.88
164	7.5554	2.592	2.646	0.069	14.43
165	6.9609	2.653	2.421	0.067	13.52

2.3 Al-clad U-10Mo-Zr Mini-plates

Two low-power U-10Mo-Zr mini-plates were selected to demonstrate the caustic dissolution of the Al cladding and the subsequent dissolution of the bare foil. The characteristics of the mini-plates are summarized in Table 2-3. The cladding was fabricated from an Al-6061 alloy.

Table 2-3. U-10Mo-Zr Mini-plate Characteristics

Mini-plate ID	A2C116	A2C117
Total Mass (g)	23.007	22.936
Foil Mass⁽¹⁾ (g)	17.41	17.25
U Enrichment⁽¹⁾ (%)	19.838	19.838
U-total Mass⁽¹⁾ (g)	15.12	14.98
U-235 Mass⁽¹⁾ (g)	3.00	2.97
Zr Mass (g)	0.62	0.61
Al Mass (g)	5.60	5.69
Mo Mass (g)	1.68	1.66

(1) Information provided by BWXT

Mini-plate A2C116 was prepared for dissolution experiments by cutting into four pieces of approximately the same size using a low speed saw. Mini-plate A2C117 was cut in half using the same low speed saw. The masses and dimensions of the mini-plate pieces are provided in Table 2-4.

Table 2-4. Masses and Dimensions of Cut U-10Mo-Zr Mini-plates

Piece ID	Mass (g)	Length (cm)	Width (cm)	Thickness (cm)
A2C116-1	5.4113	2.490	2.544	0.124
A2C116-2	6.7589	2.545	2.603	0.123
A2C116-3	6.0932	2.547	2.355	0.123
A2C116-4	4.4602	2.546	2.588	0.123
A2C117-1	10.4849	4.906	2.544	0.124

2.3.1 Al Cladding Removal

The dissolution flowsheet for the removal of the Al cladding was based on the process used at the SRS's F-Canyon facility to remove Al-6063 cladding from natural and depleted U targets used for Pu production.¹⁰ A minimum of 1.65 moles of NaOH per mole of Al was used in F-Canyon to reduce the rate of precipitation of $\text{Al}_2\text{O}_3 \cdot 3\text{H}_2\text{O}$ by the hydrolysis of NaAlO_2 (equation 6).



This amount of NaOH is about 130% excess over that required for complete dissolution of the Al. The mole ratio of NaNO_3 to Al used in the flowsheet to suppress the formation of H_2 was nominally 1.25:1. To deacid the mini-plate pieces, we targeted 1.69 moles of NaOH and 1.26 moles of NaNO_3 per mole of Al to be consistent with the F-Canyon flowsheet values.

2.3.2 Dissolution U-10Mo-Zr Foil Following Cladding Removal

To demonstrate the dissolution of the U-10Mo-Zr foil following cladding removal, a piece of the mini-plate which was cut into four pieces (Table 2-4) was dissolved using conditions demonstrated for the unclad foil (Section 2.2). The dissolution was performed targeting a terminal U concentration of 20 g/L using 4 M HNO_3 . A small amount of fluoride (as KF) was added to the solution targeting a 4 to 1 mole ratio of fluoride to Zr to address the potential presence of UZr_2 solids. The solution was heated to its boiling point.

2.4 Dissolving System

Small-scale dissolution experiments were performed using laboratory-scale glassware similar to the equipment shown in Figure 2-2. The dissolving vessel was fabricated from a 300-mL round-bottom flask (or a modified 300 mL flask with a 150-mL or a 600-mL beaker attached to the bottom – see Figure 2-3). Penetrations were added for a condenser, reagent addition, thermocouple, and gas purge. The bottom of the flask was flattened slightly to facilitate heating and agitation using a hot plate/stirrer with a magnetic stir bar. During dissolution, metal coupons were charged to the dissolver in a glass basket suspended by a glass rod which is held in place by a compression fitting. The compression fitting allows adjustment of the basket height during dissolution. The solution temperature was controlled using an external thermocouple monitored by the hot plate.

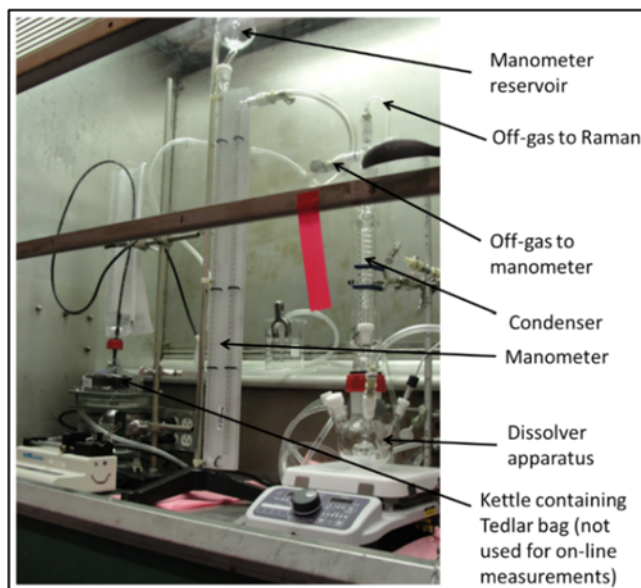


Figure 2-2. Dissolver Setup with Online Raman Offgas Analyzer

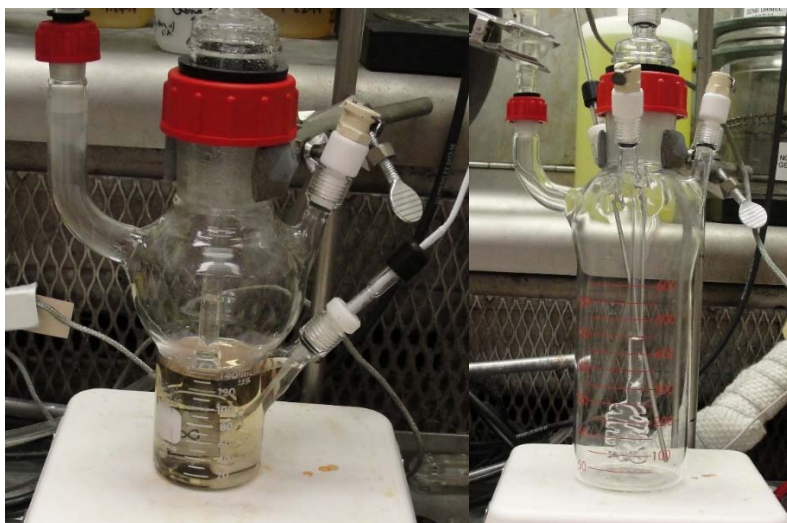


Figure 2-3. Alternate Dissolver Apparatus (left 150-mL Vessel and right 600-mL Vessel)

Offgas exiting the dissolving vessel was sampled for analysis by Raman spectroscopy using a sample line connected to a port just above the condenser. Chilled water (at 3-4 °C) was circulated through the condenser during the dissolution to remove water vapor from the offgas stream. The offgas leaving the condenser passed through a cell containing a Raman probe and terminated in a bubbler (beaker containing 700 mL or 3.5 in. of deionized water). The Raman spectrometer was used to measure non-condensable gases such as H₂, N₂, O₂, CO₂, NO, N₂O, and NO₂ in real time during an experiment. A known flowrate of CO₂ was added to the dissolving vessel during a dissolution to determine the offgas generation rate using the measured concentration of CO₂ in the offgas stream. A manometer, also connected to the offgas sample port, was used as a pressure relief device and provided a measure of the system pressure. The bubbler prevented air in-leakage from the vent side of the system.

The laboratory equipment used for the flowsheet development was designed to measure dissolution rates by taking advantage of the removable glass basket. To measure the dissolution rate of a U-10Mo coupon, the sample was placed in the perforated glass basket and suspended above the solution. The solution was heated to the desired temperature (e.g., boiling). Once at temperature, the basket containing the sample was lowered until it was completely immersed. A timer was started to record the time the sample went into the solution. At the desired interval, the basket was raised out of the solution, the timer stopped, and the basket removed from the dissolving vessel. The sample was removed from the basket, rinsed, dried, and weighed, and the dimensions measured. The sample was then returned to the basket and the basket lowered back into the solution. The timer was started again. This process was repeated until the sample was too small to remove and acquire meaningful data or sufficient data was acquired to accurately calculate the dissolution rate. The dissolution rate was calculated as the rate of change of the mass-to-surface area ratio as a function of time.

2.4.1 Raman Spectrometer

The Raman spectrometer is a GasRaman NOCH-1 spectrograph with a 532 nm DPSS laser, a high Rayleigh rejection fiber optic probe, and a high-resolution spectrometer achieving up to ~8 cm⁻¹ average optical resolution with spectral coverage from ~250 to 4,200 cm⁻¹. The Raman non-intrusively analyzes the offgas from a dissolution experiment through a quartz window using the excitation of a laser passing through a fixed portion of the offgas stream. The Raman scattering technique identifies and measures the concentration of gases in the offgas stream. The Raman spectrometer was also calibrated using the standard gases shown in Table 2-5. The Raman spectrometer measures the concentrations of the offgas species

approximately every 12-13 seconds. Since the Raman spectrometer directly measures the concentrations in the offgas stream, there is zero dead time between the offgas concentration measurement and the reading other than the analysis time of 12-13 seconds. The Raman spectrometer was controlled by and data was logged using a computer running EZRamanReader v8.3.9 software and an Excel spreadsheet.

Table 2-5. Calibration Gases for MS and Raman Analyzers

Supplier	Gas	Ar	N ₂	N ₂ O	NO ₂	NO	O ₂	H ₂
		(%)	(%)	(%)	(%)	(%)	(%)	(%)
Air Liquide	20% N ₂ O-80% Ar	80.00	—	20.00	—	—	—	—
Liquid Technology	5% NO ₂ -20% O ₂ -75% Ar	74.89	—	—	4.98	—	20.13	—
Air Liquide	20% NO-80% Ar	80.00	—	—	—	20.00	—	—
Air Liquide	5% N ₂ -10% H ₂ -85% Ar	85.00	5.00	—	—	—	—	10.00
SRNL	Ar ⁽¹⁾	99.9	—	—	—	—	—	—
SRNL	N ₂ ⁽¹⁾	—	99.9	—	—	—	—	—
SRNL	Air ⁽¹⁾	0.94	78.03	—	—	—	20.99	—

(1) Purity was not measured; the Ar was supplied from SRNL facility gases

To calculate offgas generation rates in experiments in which the Raman spectrometer was used to characterize the offgas, a CO₂ tracer gas was metered into the system through a flow controller at a set rate (nominally 20 cm³/min @ 70 °F, 1 atm). The total offgas rate was then calculated by dividing the set input rate by the measured CO₂ concentration in the offgas.

2.4.2 Raman Spectrometer Calibration and Sampling Method

The Raman spectrometer was calibrated using a set of calibration gases as shown in Table 2-5. Due to the nature of the Raman technique, the instrument only needs to be calibrated once for the intensities (or quantities) of the calibration gases. The wavelengths for the various calibration gases are known and also remain fixed. As an additional check before and after each experiment, air, 99.9 vol % CO₂, and/or a 2.67 vol % H₂ gas (balance Ar) were analyzed using the Raman spectrometer to ensure the calibration was still good. If the calibration checks were off for these gases, the Raman calibration model was adjusted for those gases after the run.

The Raman data should be positive and sum to 100% except for the 2.67 vol % H₂ gas which is 97.33 vol % Ar (which is not detected by the Raman spectrometer). Due to the noise in the Raman signal, raw readings that are less than zero are fixed to zero. In addition, the raw readings were re-baselined to zero by subtracting out average values representing zero. The gas readings for H₂, NO₂, N₂, O₂, N₂O, NO, CO₂, CO, H₂O, and NH₃ are then normalized to 100% except for the 2.67 vol % H₂ gas.

The total offgas flow is calculated from the fixed normalized sum of the CO₂ and CO concentrations divided into the CO₂ tracer flow rate coming into the system. The noise in the concentrations measured by the Raman spectrometer propagates into the total offgas flow rate so moving averages of the total offgas flow rates were performed using equation 7:

$$\text{Offgas flow rate } t_i (\text{cm}^3/\text{min}) = \frac{\sum_{k=t_i-1}^{t_i+1} \text{Offgas flow rate}_k}{3} \quad (7)$$

where Offgas flow rate = offgas generated by the dissolution in cm³/min

t_i = time at integer time step i

k = integer time step t_{i-1}, t_i, and t_{i+1}

To estimate the variability of the concentrations measured by Raman spectroscopy, the pre-run check values were compared to the standard values for all the experiments. The standard deviations of the measured concentrations with respect to the calibrated concentrations for the data were calculated. These standard deviations were then doubled to get an idea of the variability in the Raman spectroscopy concentration measurements. Table 2-6 shows the standard deviation of the measured concentrations with respect to their calibrated values. For the H₂ gas, the 2σ values or twice the standard deviation is < 0.66 vol %. The 2σ values for CO₂, O₂ and N₂ are < 3.4 vol %.

Table 2-6. Standard Deviation of Raman Concentrations with Respect to Calibrated Values

Gas	Standard Deviation (σ) (vol %)	2xStandard Deviation (2σ) (vol %)
CO ₂	1.68	3.36
N ₂	1.54	3.08
O ₂	1.04	2.08
H ₂	0.33	0.66

2.5 Quality Assurance

A Functional Classification of Safety Significant was applied to this work. Analytical measurement systems with a General Service functional classification were used to collect data during the development of flowsheet(s) for the dissolution of U-10Mo-Zr foil and Al-clad U-10Mo-Zr mini-plates. Chemical reagents used in experiments and sample preparation were purchased at levels 2 or 3. Standards used for analytical measurements were traceable to NIST or equivalent per manual 1Q, 2-7 section 5.2.3.

To match the requested functional classification, this report received technical review by design verification. Requirements for performing reviews of technical reports and the extent of review are established in manual E7, 2.60. SRNL documents the extent and type of review using the SRNL Technical Report Design Checklist contained in WSRC-IM-2002-00011, Rev. 2.

3.0 Results and Discussion

3.1 U-10Mo-Zr Foil

3.1.1 Effect of HNO₃ on Foil Dissolution

The solubility experiments were performed at the boiling point of the dissolving solution (Table 3-1) by setting the hot plate to 115 °C and then recording the boiling point measured by the hot plate thermocouple. The experiments performed at 20 g/L U with 0.05 M fluoride and 50 g/L U with 0.1 M fluoride and 0.5 M Fe using 4 and 5 M HNO₃ did not show any evidence of precipitates. Experiment 156 performed at 20 g/L U using 3 M HNO₃ formed a reddish precipitate that was easily re-suspended upon shaking (Figure 3-1). After about a week, some of the reddish solids re-settled (less than what was originally present) and then after about another week, the amount of settled solids was reduced even more (Figure 3-2). An attempt was made to isolate the solids but during handling of the bottle, the solids dissolved. In order to identify the reddish solids, an additional experiment would have to be performed using 3 M HNO₃ to dissolve a piece of the U-10Mo-Zr foil in an attempt to precipitate and isolate the solids. In previous dissolution experiments using U-Mo foils, researchers at ANL reported the formation of an orange-red precipitate, but were not able to identify solids due to the formation of such a low mass and the subsequent re-dissolution.^{6,5}

Table 3-1. Boiling Points for Dissolved Foil Solubility Experiments

Experiment	Boiling Point (°C)
156	101
157	101
158	102
161	102
162	103
163	103

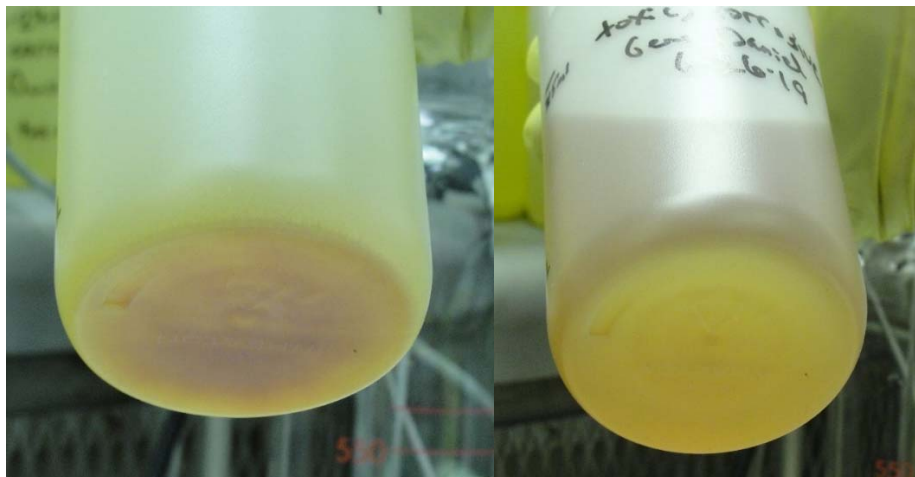


Figure 3-1. Exp 156 Solution After 1 day Settling (left) Before Mixing and (right) After Mixing



Figure 3-2. Exp 156 Solution After 12 days Settling (left) and 21 days Settling (right)

The experiment performed at 50 g/L U using 3 M HNO₃ containing 0.1 M fluoride and 0.5 M Fe resulted in the formation of a white-looking precipitate which stuck to the side of the vessel (Figure 3-3). The precipitate was submitted for x-ray diffraction (XRD) and was identified as a Zr-Mo compound (ZrMo₂O₅(OH)₂(H₂O)₂) (Figure 3-4). There were no U products identified in the precipitate by XRD.



Figure 3-3. Exp 161 Solution After Cooling – White Solids on Glassware

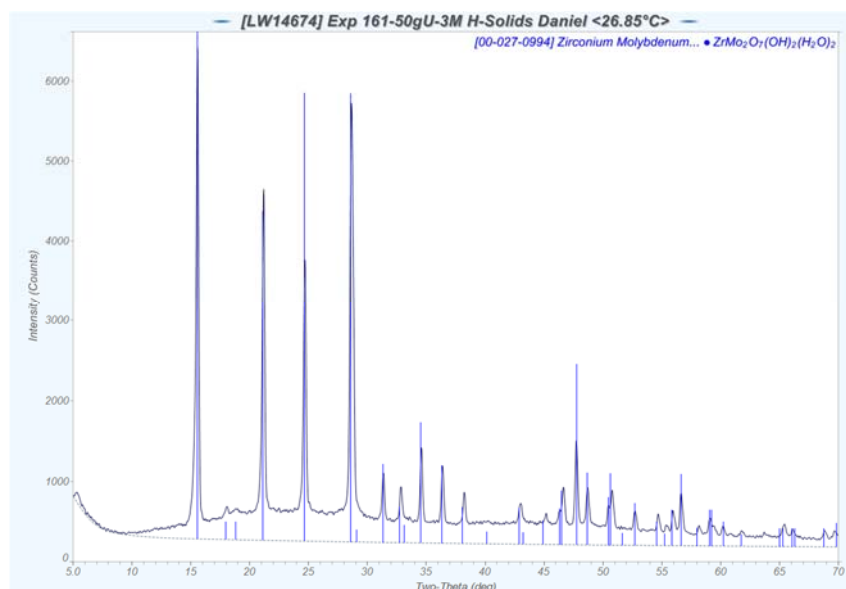


Figure 3-4. XRD of Exp 161 Precipitate – 50 g/L U, 3 M HNO₃, 0.1 M Fluoride, and 0.5 M Fe

Based on the experiments discussed above, the starting HNO₃ concentration must result in a final acid concentration greater than approximately 3.5 M for both terminal U concentrations investigated to prevent the formation of solids. Below this concentration the formation of a Zr-Mo precipitate is likely at 50 g/L U and a transient reddish solid is formed (which subsequently re-dissolves) at 20 g/L U. Therefore, the use of a sufficient volume of 4 M HNO₃ resulting in a final acid concentration greater than approximately 3.5 M is recommended to dissolve the U-10Mo-Zr foil. The fluoride concentration should be adjusted to establish a 4:1 mole ratio of fluoride to Zr and 0.5 M Fe (as Fe(NO₃)₃) added to the solution for a final target U concentration of 50 g/L.

As another check of the final solutions from the solubility experiments, the K, Zr, and U were analyzed by inductively-coupled mass spectrometry (ICPMS) and compared with estimated values based on the composition and masses of the foils. Table 3-2 shows the ICPMS results from the 6 foil dissolution experiments along with their estimated values. Within analytical ($\pm 20\%$) and volume measurement ($\pm 10\%$) uncertainties, the measured and estimated values are consistent.

Table 3-2. Composition of Dissolving Solutions from Foil Solubility Experiments

Experiment	Measured K (M)	Estimated K (M)	Measured Zr (g/L)	Estimated Zr (g/L)	Measured U (g/L)	Estimated U (g/L)
156	0.05	0.05	0.83	0.89	19.4	20.26
157	0.05	0.05	0.82	0.89	19.5	20.27
158	0.05	0.05	0.78	0.89	19.6	20.27
161	0.1	0.1	2.03	2.25	51.8	51.21
162	0.09	0.1	1.91	2.25	52.4	51.16
163	0.11	0.1	2.10	2.25	50.4	51.15

3.1.2 Dissolution Rate of Foil

Dissolution rates for U-10Mo-Zr foil coupons were calculated from the slopes of linear fits to the mass-to-surface area ratio versus dissolution time data. These data are discussed in this section for Experiment 159 with a target 20 g/L U concentration using 4 M HNO₃ containing 0.05 M fluoride and Experiment 164 with a target 50 g/L U concentration using 4 M HNO₃ containing 0.1 M fluoride and 0.5 M Fe.

Data (Experiment 159) for the dissolution experiment targeting 20 g/L U are shown in Table 3-3. Two linear fits of the mass-to-surface area ratio versus dissolution time data were performed as shown in Figure 3-5. It is believed that the initial linear fit (with an order of magnitude lower slope than the second linear fit) is due to the dissolution of the (exterior) Zr diffusion barrier on the U-10Mo foil. Once the Zr cladding is breached or dissolved, the dissolution rate increases an order of magnitude. The initial dissolution rate was $-5.58\text{E-}03$ g/cm²/min with a standard deviation of $2.43\text{E-}03$ and an R² equal to 0.85. The second dissolution rate was $-1.20\text{E-}02$ g/cm²/min with a standard deviation of $3.93\text{E-}04$ and an R² equal to 0.997. The initial dissolution rate with $\pm 2\sigma$ variance ranges from $1.0\text{E-}03$ to $1.1\text{E-}02$ g/cm²/min which is close to the $\pm 2\sigma$ range of the second slope of $1.1\text{E-}02$ to $1.3\text{E-}02$ g/cm²/min. Therefore, the initial rate may not be distinguishable from the second rate. The second dissolution rate closely matches prior dissolution rates measured for LEU with about 20% enrichment¹⁷ of $1.16\text{E-}02$ g/cm²/min which suggests the 10 wt % Mo has little effect on the dissolution rate of the alloy at these conditions.

Table 3-3. Experiment 159 – Dissolution Data for U-10Mo-Zr foil at 20 g/L U

Dissolution Time (min)	Mass (g)	Estimated Dissolved U (g/L)	Length (mm)	Width (mm)	Diameter (mm)	Surface Area (cm ²)	Mass/SA (g/cm ²)
0	7.9051	0.00	22.64	30.92	0.69	14.74	0.536
5.12	7.4189	1.42	23.36	31.17	0.68	15.30	0.485
10.20	6.9516	2.79	30.81	22.51	0.68	14.59	0.476
15.27	6.1087	5.25	30.69	22.26	0.58	14.28	0.428
20.30	5.0541	8.34	30.73	22.20	0.5	14.17	0.357
25.33	4.0546	11.26	30.35	21.91	0.48	13.80	0.294
30.47	3.1050	14.04	29.09	21.67	0.38	12.99	0.239

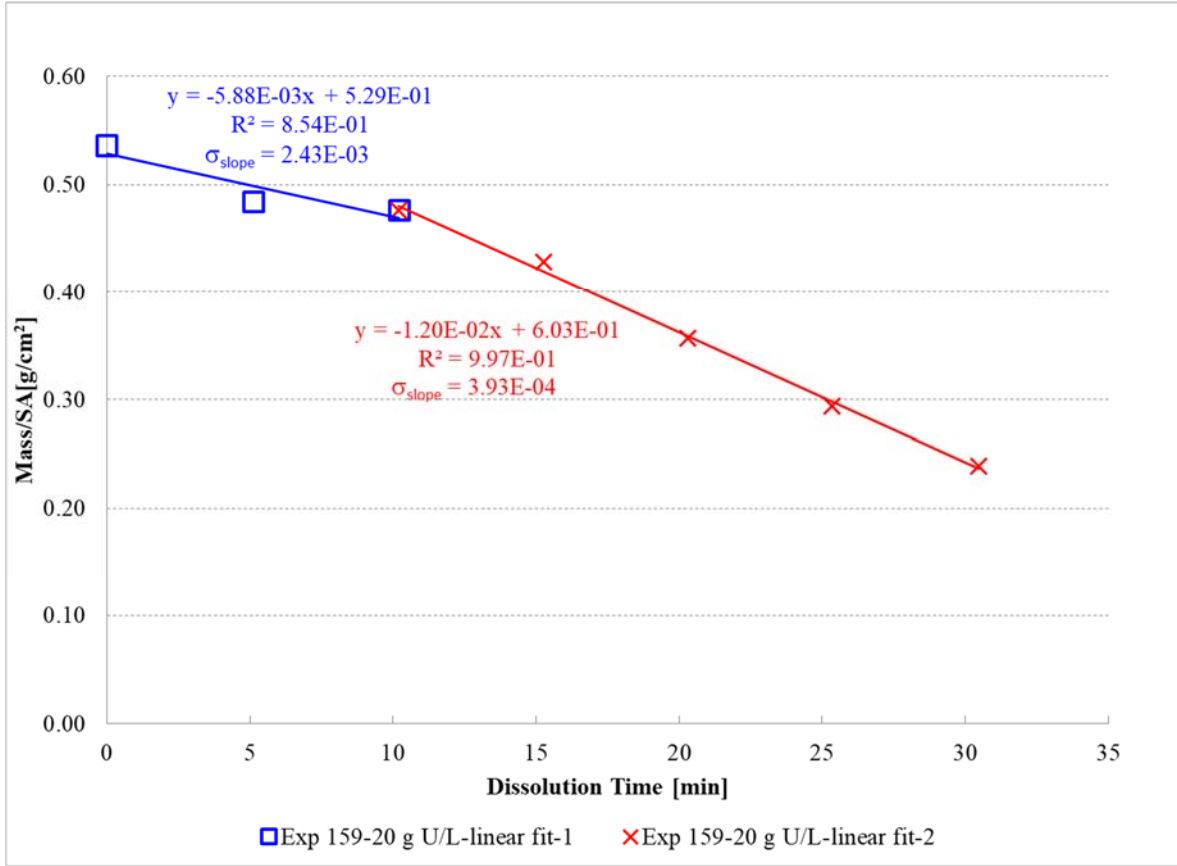


Figure 3-5. Experiment 159 – Dissolution Rates for U-10Mo-Zr foil at 20 g/L U

Data (Experiment 164) for the dissolution experiment targeting 50 g/L U are shown in Table 3-4. Two linear fits of the mass-to-surface area ratio versus dissolution time data were performed as shown in Figure 3-6. Similar to Experiment 159, it is believed that the initial linear fit with an order of magnitude lower slope than the second linear fit is due to the (exterior) Zr diffusion barrier on the U-10Mo foil. Once the Zr cladding is breached or dissolved, the dissolution rate increases an order of magnitude. The initial dissolution rate was $-3.95\text{E-}03 \text{ g/cm}^2/\text{min}$ with a standard deviation of $2.38\text{E-}04$ and an R^2 equal to 0.99. The second dissolution rate was $-1.50\text{E-}02 \text{ g/cm}^2/\text{min}$ with a standard deviation of $1.87\text{E-}03$ and an R^2 equal to 0.97. The initial dissolution rate with $\pm 2\sigma$ variance ranges from $3.5\text{E-}03$ to $4.4\text{E-}03 \text{ g/cm}^2/\text{min}$ which is statistically different than the $\pm 2\sigma$ range of the second slope of $7.5\text{E-}03$ to $2.2\text{E-}02 \text{ g/cm}^2/\text{min}$. Consistent with the Experiment 159 results, it appears that there is an initial slower rate due to the Zr cladding. To illustrate this point, the progressive removal of the Zr diffusion barrier can be seen in Figure 3-7 for Experiment 164. The second dissolution rate closely matches prior dissolution rates measured for LEU from the Idaho National laboratory¹⁷ which is consistent with Experiment 159.

Table 3-4. Experiment 164 – Dissolution Data for U-10Mo-Zr foil at 50 g/L U

Dissolution Time (min)	Mass (g)	Estimated Dissolved U (g/L)	Length (mm)	Width (mm)	Diameter (mm)	Surface Area (cm ²)	Mass/SA (g/cm ²)
0	7.5554	0.00	25.92	26.46	0.69	14.43	0.523
5.05	7.2297	0.95	25.88	26.41	0.72	14.42	0.501
10.05	6.9206	1.86	25.83	26.35	0.71	14.34	0.483
15.05	6.6096	2.77	25.62	26.30	0.68	14.17	0.466
19.98	6.2382	3.85	25.36	25.89	0.67	13.82	0.451
24.97	5.7324	5.33	25.09	25.96	0.66	13.70	0.419
30.10	5.0098	7.44	24.53	25.68	0.65	13.25	0.378
35.05	4.1052	10.09	24.54	23.78	0.64	12.29	0.334
40.03	2.991	13.35	23.74	23.25	0.60	11.60	0.258
45.00	1.6741	17.20	23.07	22.54	0.46	10.81	0.155

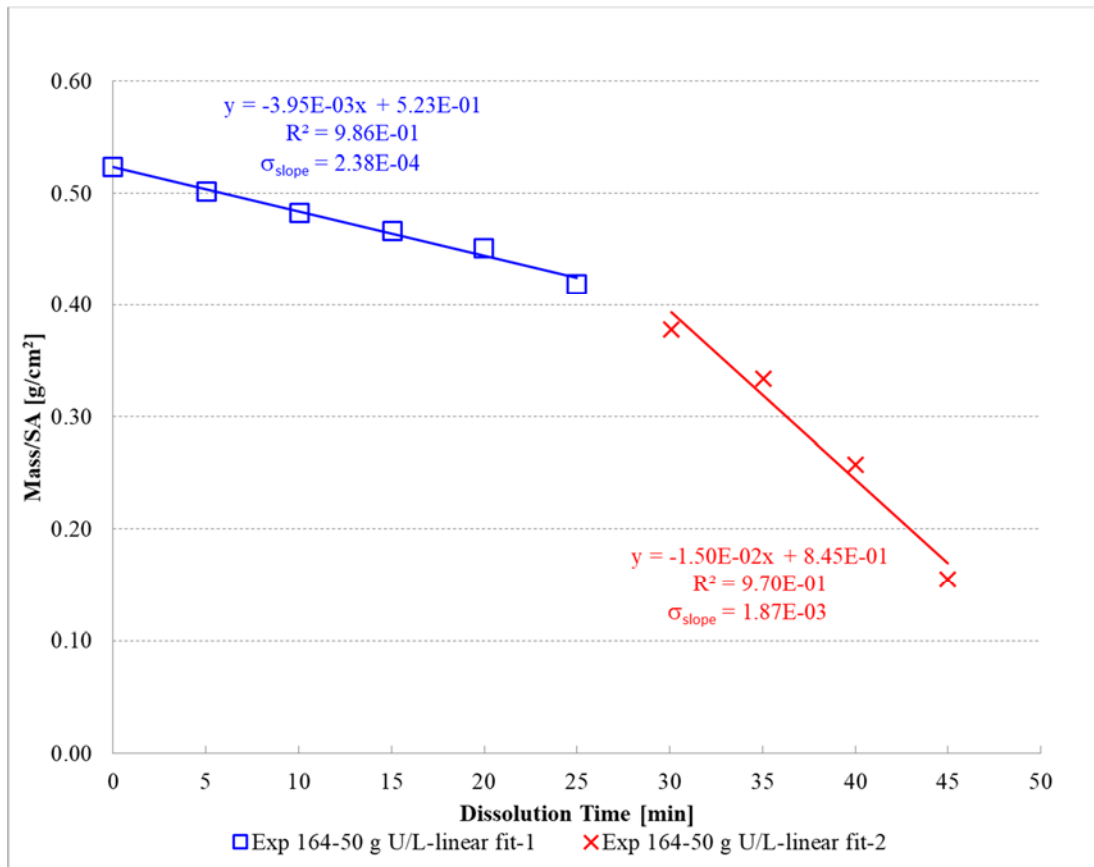


Figure 3-6. Experiment 164 – Dissolution Rates for U-10Mo-Zr foil at 50 g/L U

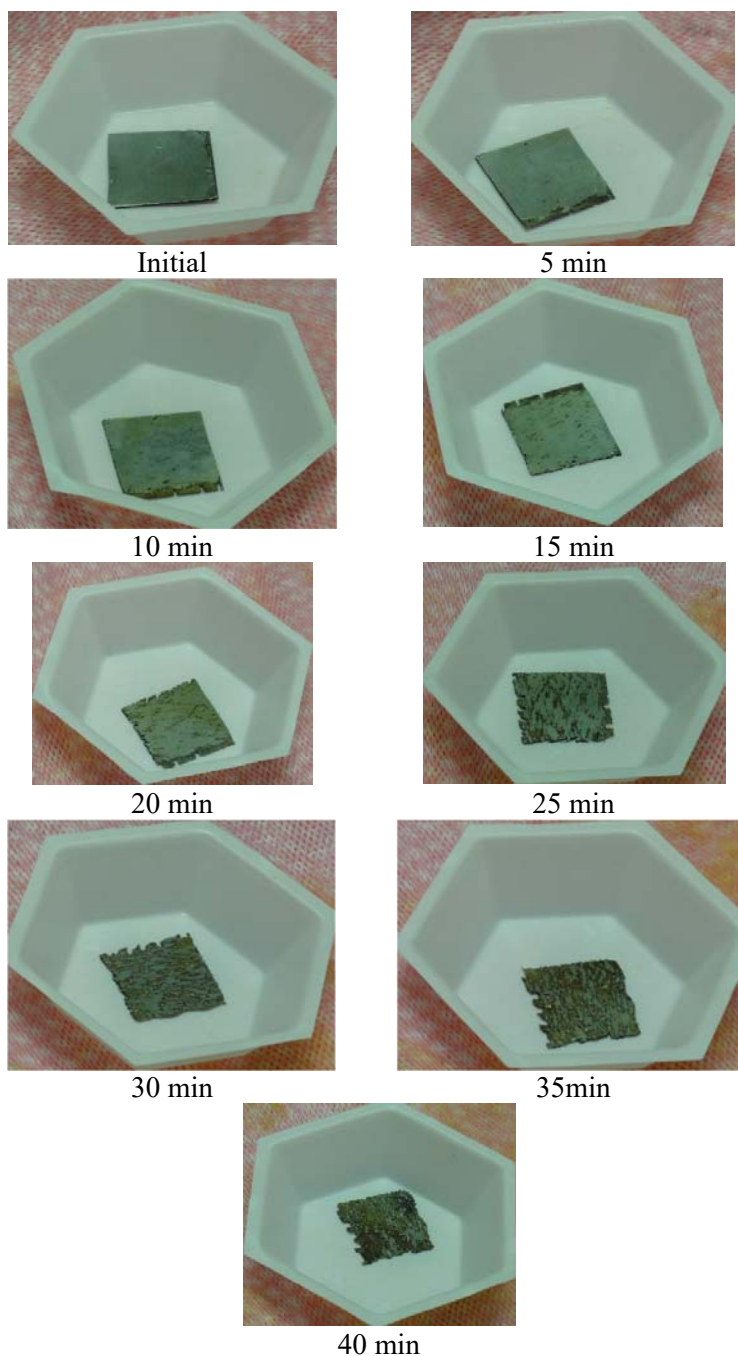


Figure 3-7. Experiment 164 – Progressive Removal of Zr Diffusion Barrier

3.1.3 Characterization of Offgas During Foil Dissolution

The offgas generation rates for Experiment 160 in which a U-10Mo-Zr foil was dissolved in 4 M HNO₃ to a final U concentration of 20 g/L is shown in Figure 3-8. The peak total offgas rate was about 2.6 cm³/min/cm² with approximately 2.3 cm³/min/cm² of NO, 0.2 cm³/min/cm² of NO₂, 0.06 cm³/min/cm² O₂, 0.02 cm³/min/cm² of H₂, 0.02 cm³/min/cm² of N₂O, and 0.01 cm³/min/cm² N₂. The bulk of the gas produced was NO and NO₂.

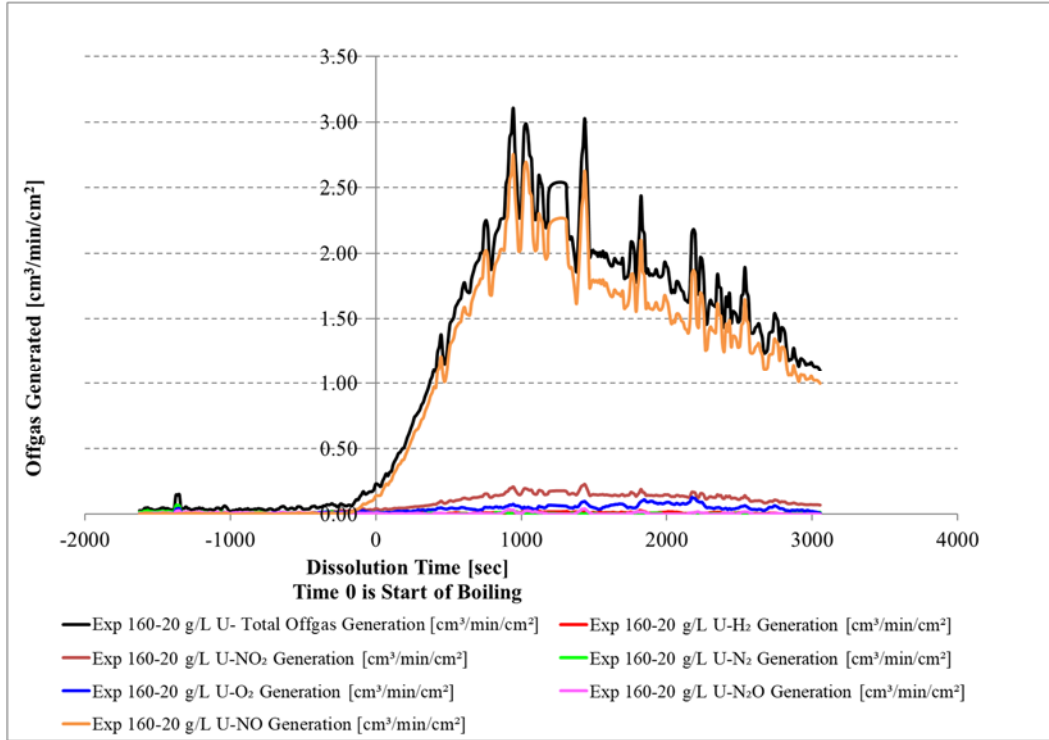


Figure 3-8. Exp 160 Offgas Generation Rates from the Dissolution of U-10Mo-Zr Foil in 4 M HNO₃ and 0.05 M Fluoride to a Final U concentration of 20 g/L

The offgas generation rates for Experiment 165 in which a U-10Mo-Zr foil was dissolved in 4 M HNO₃ to a final U concentration of 50 g/L is shown in Figure 3-9. The peak total offgas rate was about 4.6 cm³/min/cm² with approximately 3.3 cm³/min/cm² of NO, 0.8 cm³/min/cm² of NO₂, 0.4 cm³/min/cm² O₂, 0.09 cm³/min/cm² of H₂, 0.04 cm³/min/cm² of N₂O, and 0.00 cm³/min/cm² N₂. The bulk of the gas produced was NO and NO₂ which is consistent with Experiment 160.

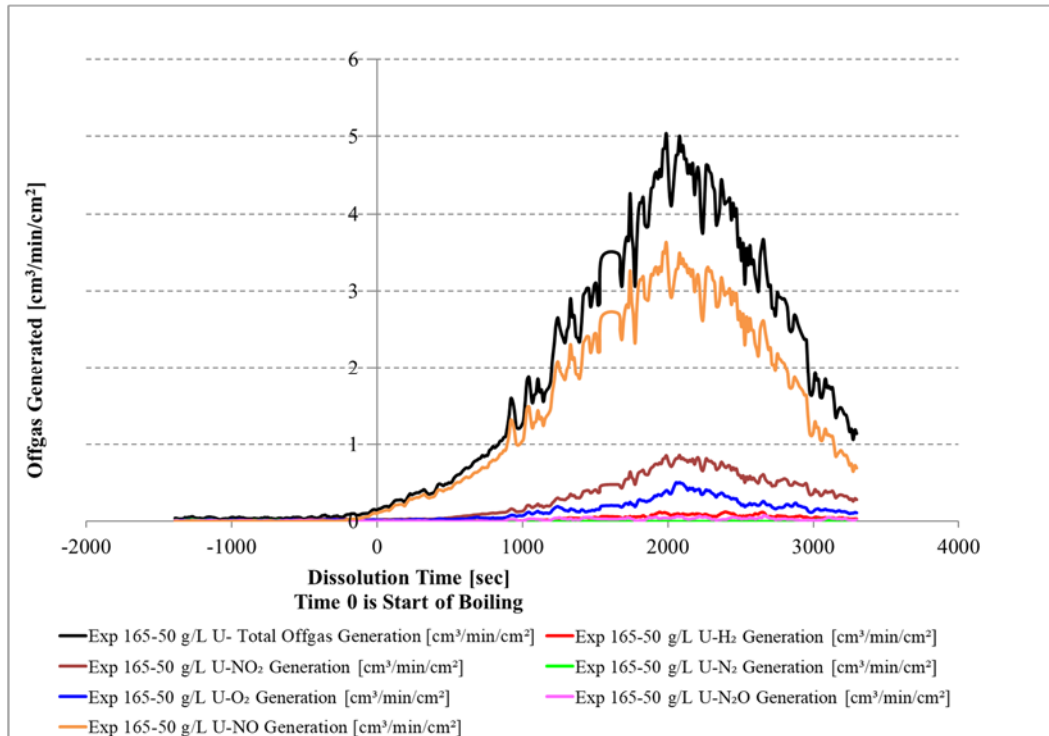


Figure 3-9. Exp 165 Offgas Generation Rates from the Dissolution of U-10Mo-Zr Foil in 4 M HNO₃ and 0.1 M Fluoride to a Final U concentration of 50 g/L

The rate of H₂ gas generation from the dissolution of the U-10Mo-Zr foil could be a potential flammability concern so the H₂ generation rate was quantified. An expanded perspective of the H₂ generation rates for Experiment 160 and 165 are plotted as a function of time in Figure 3-10. The H₂ generation rates were calculated from the measured offgas generation rates, measured H₂ concentrations, and the measured surface area of the U-10Mo-Zr foils. Time zero corresponds to the start of boiling but offgas generation was measured from the point the foil was immersed in the solution at room temperature and during solution heating. The figure shows that the H₂ generation rates increase once the boiling point of the solution was reached. Experiment 165 had a higher H₂ generation rate peaking at about 0.09 cm³/min/cm² while Experiment 160 had a lower H₂ generation rate peaking at about 0.02 cm³/min/cm². Since the acid concentrations were the same in both experiments, the higher H₂ generation rate for Experiment 165 is likely attributed to the higher fluoride concentration (about twice that of Experiment 160). The H₂ generation rates are small compared to the generation rate from the Hg-catalyzed dissolution of Al (e.g., alloy Al-1100) in HNO₃ which normally peak around 2 cm³/min/cm².¹⁸

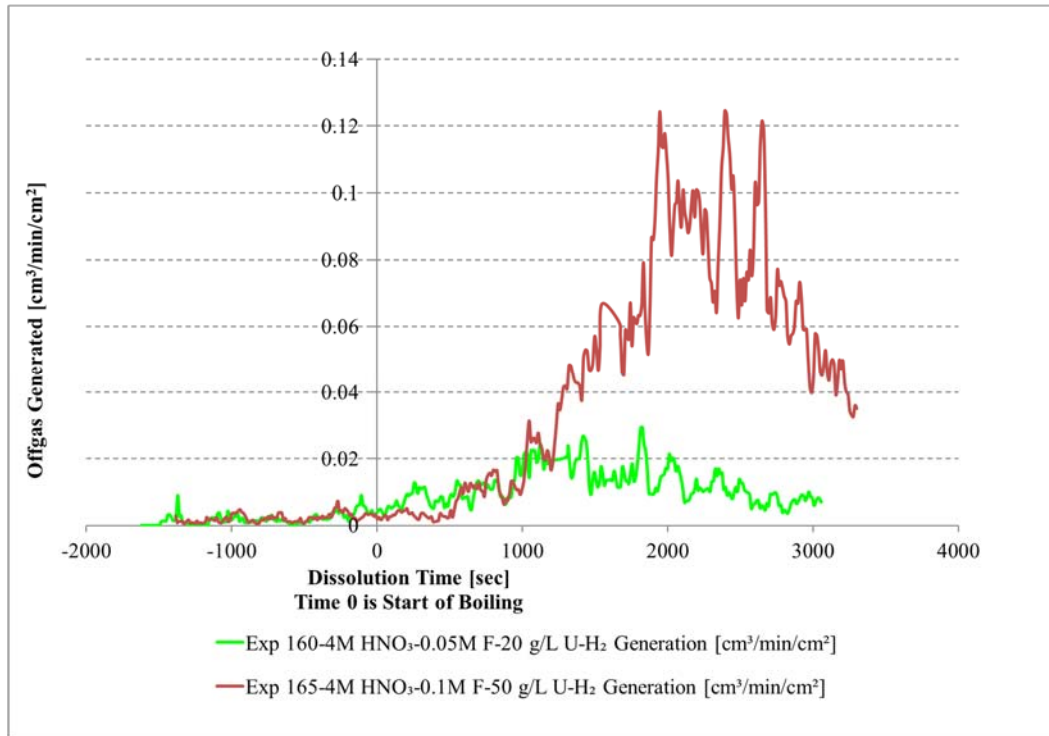


Figure 3-10. H₂ Generation Rates from the Dissolution of U-10Mo-Zr Foil

3.2 U-10Mo-Zr Mini-plate

3.2.1 Al Cladding Dissolution

Based on the process used in the F-Canyon facility for the caustic dissolution of Al-6063 cladding discussed in Section 2.3.1,¹⁰ the first decladding experiment (Experiment 166) for a piece of mini-plate A2C117 (Piece 1) was performed using 370 mL of a 0.44 M NaOH solution containing 0.33 M NaNO₃. This volume and the concentrations were based on an estimated mass of Al-6061 of 2.6 g or 0.0963 mole in the piece of the mini-plate. For 130% excess stoichiometry (as F-Canyon used), the amounts of NaOH and NaNO₃ required were approximately 0.164 and 0.122 mole, respectively, to dissolve the Al cladding. Based on the size of the 600-mL vessel and to ensure full immersion of Piece 1, a 370 mL volume of solution was used resulting in initial concentrations of NaOH and NaNO₃ of 0.44 and 0.33 M, respectively.

The offgas generation rates for Experiment 166 are shown in Figure 3-11. The peak total offgas rate was about 0.14 cm³/min/cm² with approximately 0.11 cm³/min/cm² of H₂, 0.02 cm³/min/cm² N₂, 0.01 cm³/min/cm² O₂, and 0 cm³/min/cm² of NO, NO₂, N₂O, and NH₃. The bulk of the gas produced was H₂. The experimental plan was to monitor the H₂ offgas generation as an indicator of when the decladding was complete (Figure 3-12 shows an expanded view of just the H₂ generation rate). The H₂ offgas indicated that reaction started before boiling and peaked when the boiling point of the solution was reached and then started to dissipate as expected. However, when Piece 1 was removed after 101 minutes, rinsed, and dried, it weighed 10.28 g (Figure 3-13) giving an approximate Al dissolution rate of 0.002 g/min. There were also a lot of white solids that had precipitated (Figure 3-14). The final declad foil mass should have been closer to 7.9 g. Based on these results, a decision was made to increase the NaOH concentration since it drives the Al dissolution rate.

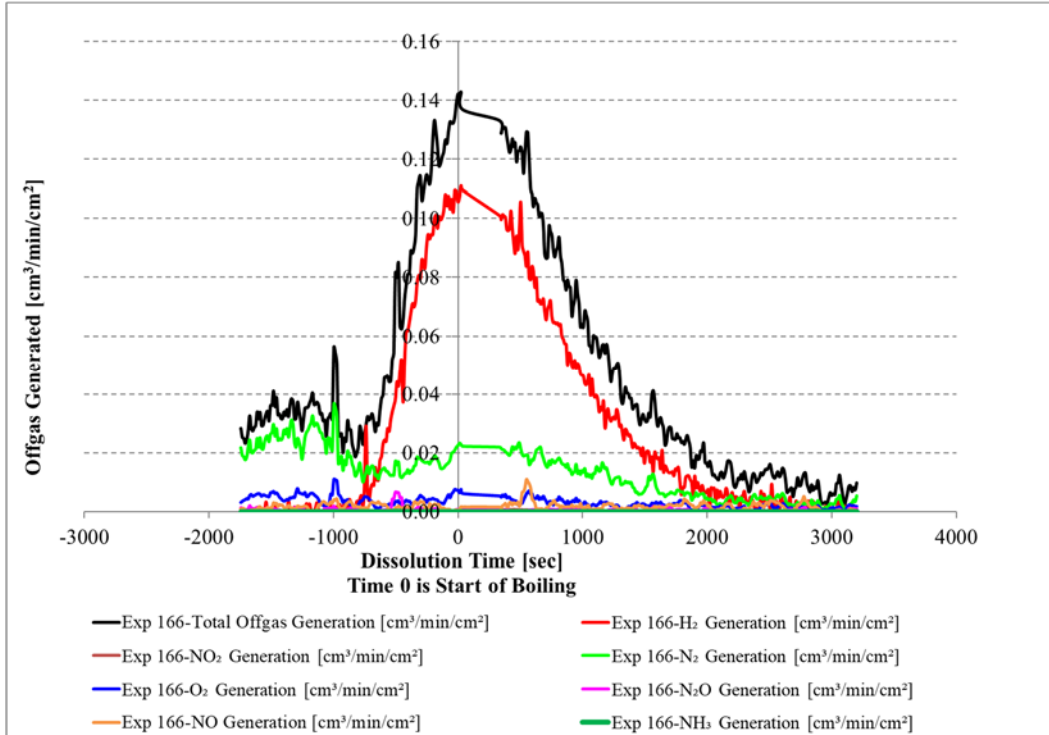


Figure 3-11. Exp 166 Offgas Generation Rates from the Caustic Partial Decladding of Piece 1 of Mini-plate A2C117 in 0.44 M NaOH and 0.33 M NaNO₃

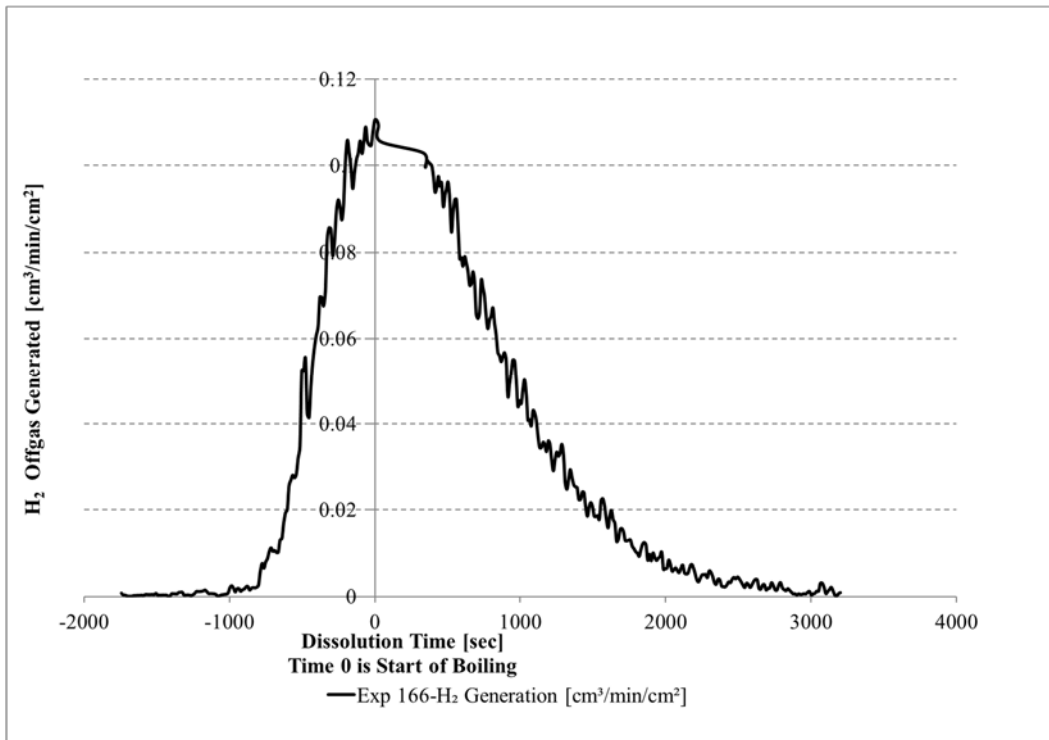


Figure 3-12. Exp 166 H₂ Generation Rate from the Caustic Partial Decladding of Piece 1 of Mini-plate A2C117 in 0.44 M NaOH and 0.33 M NaNO₃



Figure 3-13. Caustic Decladding of Piece 1 of Mini-plate A2C117 after 101 min of Boiling



Figure 3-14. White Solids from the Caustic Decladding of Piece 1 of Mini-plate A2C117

For Experiment 166B, 74 mL of 10 M NaOH solution were added to the Experiment 166 solution to bring the NaOH concentration to approximately 2 M assuming some NaOH had been used to dissolve the approximate 0.2 g of Al cladding. Since the H₂ generation did not provide an accurate indication of the completion of the Al decladding, the plan was to observe the bubbles in the reactor and when they stopped/slowed, remove the piece of the mini-plate, and measure the mass to see if the expected mass of Al had been lost. As a comparison, near the start of boiling with Piece 1 of the mini-plate in the 0.44 M NaOH, the solution looked as shown on the left side in Figure 3-15. When Piece 1 was contacted with 2 M NaOH, the solution looked as shown on the right side of Figure 3-15. There were a lot more bubbles (i.e., offgas) generated in the 2 M NaOH solution than in the 0.44 M NaOH solution and the solution was dark or black from the Al spalling-off the mini-plate piece indicating that more Al dissolution was occurring. After 20 minutes of boiling, the solution looked as though all reaction had stopped (Figure 3-16). The mini-plate was removed after 20 minutes, rinsed, and dried (Figure 3-17). The mass of Piece 1 was 7.63 g which was less than expected indicating that all the Al had probably dissolved. The approximate Al dissolution rate was 0.13 g/min or several orders of magnitude higher than measured in the solution containing 0.44 M NaOH.



Figure 3-15. Near the Start of Boiling during Decladding of Piece 1 of Mini-plate A2C117 in 0.44 M NaOH (left) and 2 M NaOH (right)



Figure 3-16. 20 min After the Start of Boiling during Decladding of Piece 1 of Mini-plate A2C117 in 2 M NaOH



Figure 3-17. Declad Piece 1 of Mini-plate A2C117

Based on the results of Experiment 166, a 100-mL dissolution of 1.678 g of Al-6061 metal was performed using a 1 M NaOH solution containing 0.75 M NaNO₃ which resulted in a measured dissolution rate of approximately 0.05 g Al/min which appeared acceptable. Another 100-mL dissolution of 1.696 g of Al-6061 metal was performed using a 2 M NaOH solution containing 1.5 M NaNO₃ which resulted in a measured dissolution rate of approximately 0.11 g Al/min which also appeared acceptable.

Using the Al-6061 dissolutions as a basis, Experiment 168 was planned to declad a 6.09 g piece of mini-plate A2C116 (Piece 3) using 100 mL of a 1 M NaOH solution containing 0.75 M NaNO₃. The offgas was monitored as well as watching the bubbles in the dissolving solution based on what was observed in Experiment 166. The offgas generation rates for Experiment 168 are shown in Figure 3-18. The peak total offgas rate was about 0.14 cm³/min/cm² with approximately 0.09 cm³/min/cm² of H₂, 0.03 cm³/min/cm² N₂, 0.01 cm³/min/cm² O₂ and N₂O, and 0 cm³/min/cm² of NO, NO₂, and NH₃. The bulk of the gas produced was H₂.

An expanded view of the H₂ offgas generation for Experiment 168 is shown in Figure 3-19. Approximately 30 minutes (1800 seconds) into boiling, the solution did not appear to be turning dark black like the solution in Experiment 166 and white flakes were forming indicating the decladding was not proceeding as expected (Figure 3-20). The H₂ offgas generation decreased to zero indicating that the decladding reaction had stopped after about 58 minutes of boiling. A decision was made to spike the solution to increase the NaOH concentration to try to restart the decladding reaction. A 6 mL aliquot of 10 M NaOH was spiked into the solution to increase the NaOH concentration to approximately 1.5 M. After the spike, the H₂ generation increased slightly then dropped and there was no visual evidence like excessive bubbling indicating that the Al dissolution had restarted. The mini-plate was removed after 77 minutes of boiling, rinsed, and dried. The mass was 5.91 g giving an approximate Al dissolution rate of 0.002 g/min. The Al decladding was not proceeding as observed in the Al-6061 dissolutions.

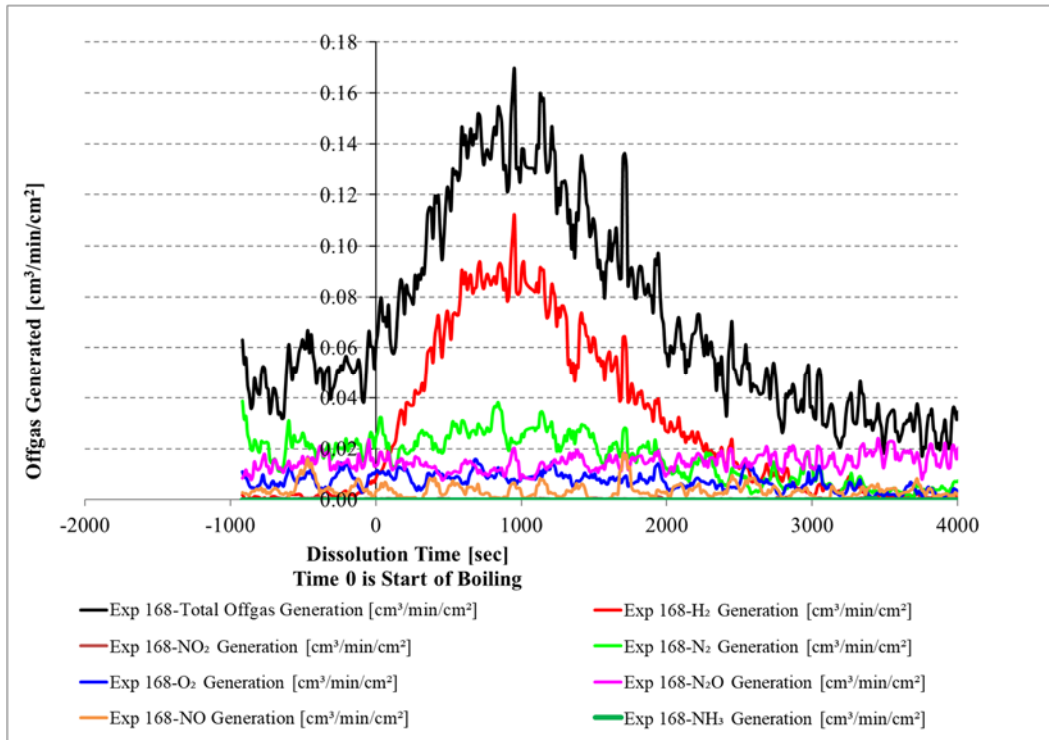


Figure 3-18. Exp 168 Offgas Generation Rates from the Partial Decladding of Piece 3 of Mini-plate A2C116 using a 1 M Solution of NaOH Containing 1.5 M NaNO₃

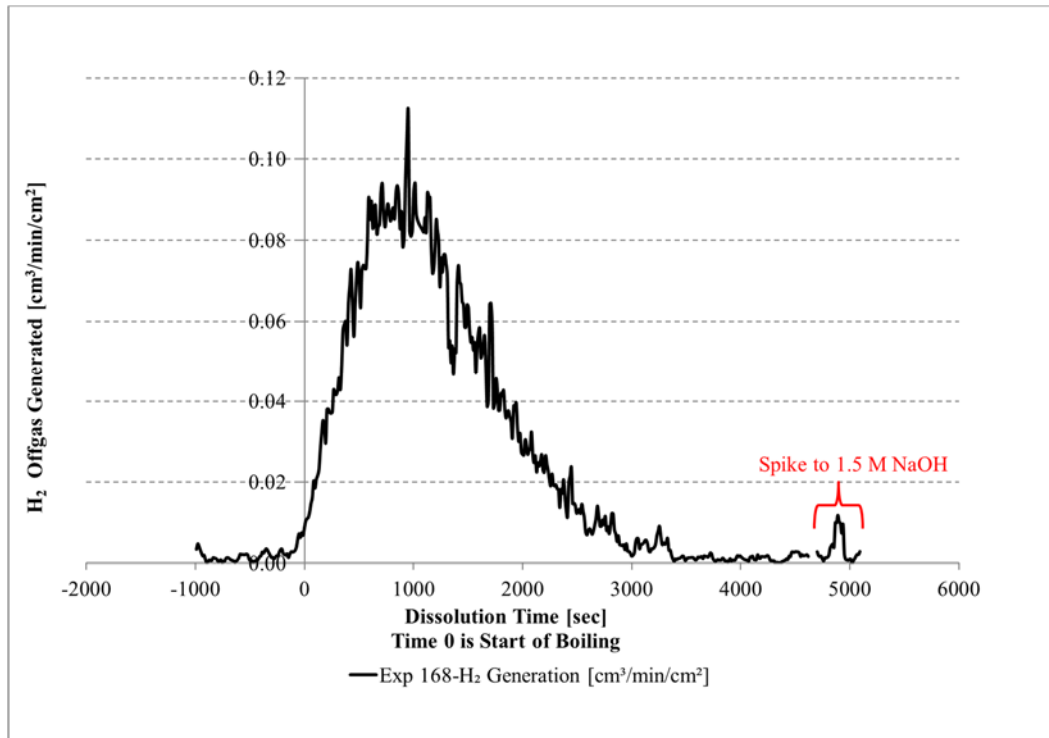


Figure 3-19. H₂ Generation Rate from the Decladding of Piece 3 of Mini-plate A2C116 using a 1 M Solution of NaOH Containing 1.5 M NaNO₃



Figure 3-20. Decladding of Piece 3 of Mini-plate A2C116 Following 30 min of Boiling in 1 M NaOH

To determine if a higher concentration of NaOH would improve the Al dissolution rate, a second decladding experiment was performed with Piece 3 of mini-plate A2C116 using 100 mL of a 2 M NaOH solution containing 1.5 M NaNO₃ (Experiment 168A). The offgas was monitored using the Raman spectrometer as well as observing the bubble formation in the solution based on what was observed in Experiment 166. The offgas generation rates for Experiment 168A are shown in Figure 3-21. The peak total offgas rate was about 0.12 cm³/min/cm² with approximately 0.07 cm³/min/cm² of H₂, 0.03 cm³/min/cm² of N₂O, 0.01 cm³/min/cm² N₂ and NO, and 0 cm³/min/cm² of O₂, NO₂, and NH₃. The bulk of the gas produced was H₂.

An expanded view of the H₂ offgas generation rate for Experiment 168A is shown in Figure 3-22. Approximately 13 minutes (780 seconds) into boiling, the solution did not appear to be turning dark black like in Experiment 166 and white flakes were forming about 29 minutes into boiling indicating the dissolution was not proceeding as expected (Figure 3-23). The H₂ offgas generation rate decreased to zero indicating that the decladding reaction had stopped after about 29 minutes of boiling. The experiment was stopped after 38 minutes of boiling and the piece of the mini-plate removed from the vessel, rinsed, and dried. The mass was 5.6558 g. The approximate Al dissolution rate in the 2 M NaOH solution containing 1.5 M NaNO₃ was 0.007 g/min or orders of magnitude lower than expected.

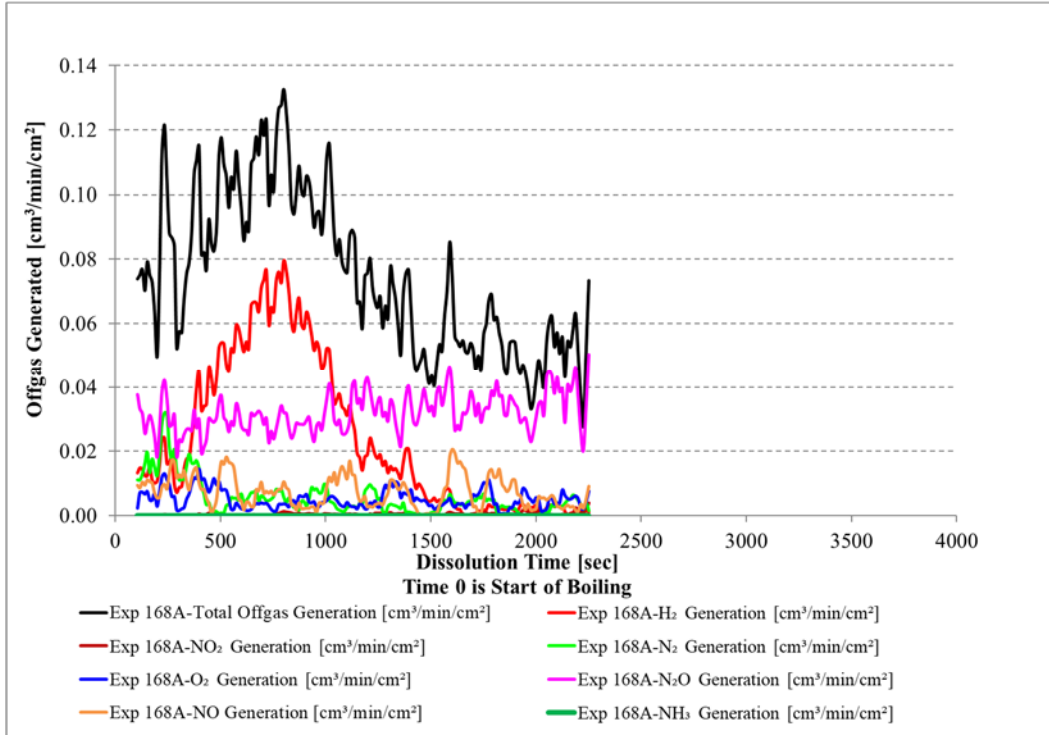


Figure 3-21. Exp 168A Offgas Generation Rates from Partial Decladding of Piece 3 of Mini-plate A2C116 using 2 M NaOH and 1.5 M NaNO₃

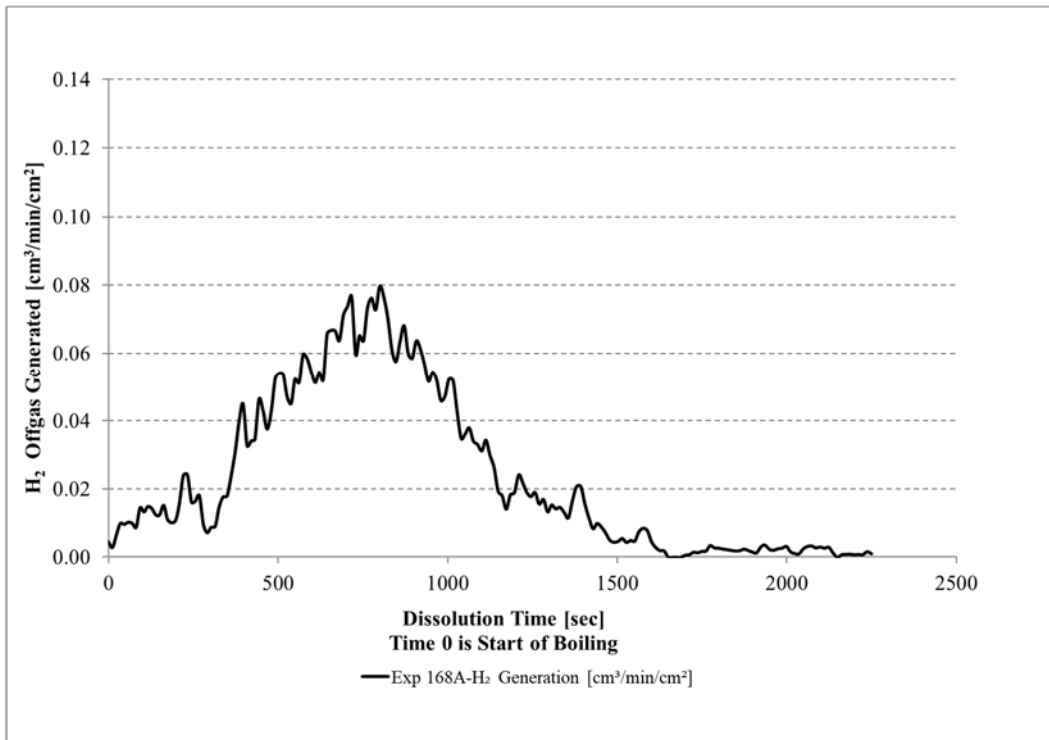


Figure 3-22. Exp 168A H₂ Generation Rate from Partial Decladding of Piece 3 of Mini-plate A2C116 using 2 M NaOH and 1.5 M NaNO₃

The white solids from Experiment 166 were analyzed by XRD (Figure 3-24) which indicated that the Al was coming back out of solution as Bayerite ($\text{Al}(\text{OH})_3$), Dawsonite ($\text{NaAlCO}_3(\text{OH})_2$), and Boehmite ($\text{AlO}(\text{OH})$). Based on the last decladding experiment, there appears to be not only an excess amount of NaOH required to dissolve the Al cladding but also an excess concentration needed to keep the dissolved Al in solution rather than precipitating as one of the Al compounds identified by XRD in Experiment 166. Based on the original F-Canyon flowsheet for 130% excess stoichiometry, 1.69 moles of NaOH and 1.26 moles of NaNO_3 per mole of Al are required. However, the experiments performed using this ratio did not completely dissolve the Al. Experiment 166B did successfully declad a piece of a U-10Mo-Zr mini-plate using 9.37 moles of NaOH and 1.27 moles of NaNO_3 per mole of Al. Using these ratios, 0.48 mole of NaOH and 0.064 mole of NaNO_3 would be needed to dissolve the estimated 1.38 g of Al cladding left on Piece 3 of mini-plate A2C116. For a volume of 200 mL, a 2.4 M NaOH solution containing 0.32 M NaNO_3 would provide the necessary moles of NaOH to finish de-cladding the piece of the mini-plate. To ensure the decladding was successful, 250 mL of a 2.6 M NaOH solution containing 0.33 M NaNO_3 was prepared for Experiment 168B.



Figure 3-23. 13 min (left) and 29 min (right) into Boiling during the Decladding of Piece 3 of Mini-plate A2C116 using 2 M NaOH

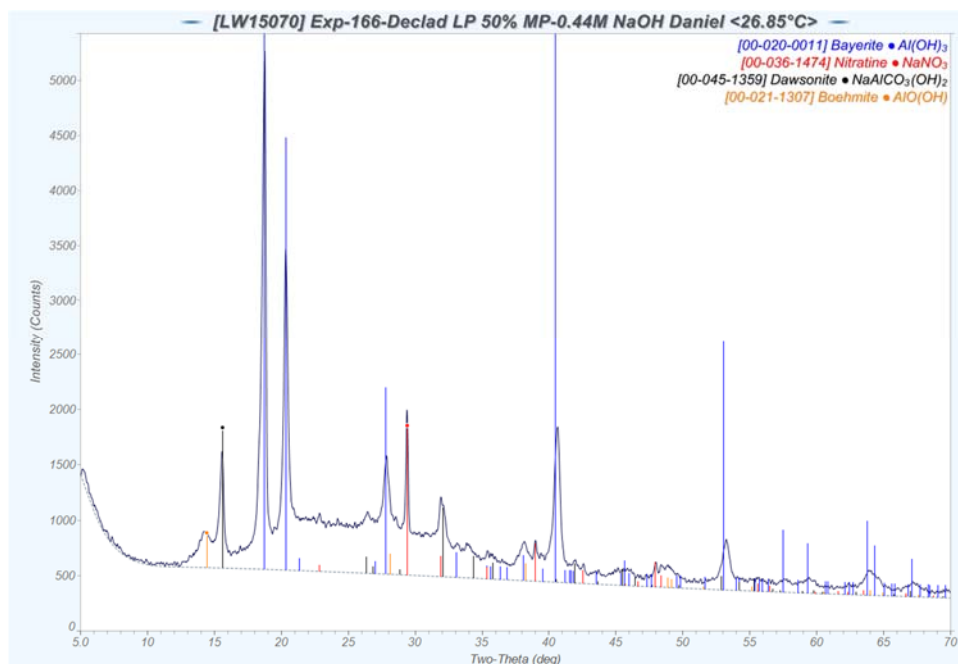


Figure 3-24. XRD of Experiment 166 Precipitate – 20 g/L U, 0.44 M NaOH, and 0.33 M NaNO₃

The partially declad Piece 3 of mini-plate A2C116 had an initial mass of 5.6558 g. Although the H₂ generation rate does not provide an accurate indication of the completion of the Al decladding, it does indicate that the decladding is proceeding. The plan for this experiment (168B) was to measure the H₂ offgas generation rate using the Raman spectrometer, observe the bubble formation in the vessel, and when the bubbles stopped/slowed, remove the mini-plate piece and measure the mass to see if the expected mass of Al had been dissolved. The offgas generation rates for Experiment 168B are shown in Figure 3-25. The peak total offgas rate was about 2.14 cm³/min/cm² with approximately 1.85 cm³/min/cm² of H₂, 0.17 cm³/min/cm² N₂, 0.08 cm³/min/cm² of O₂, 0.02 cm³/min/cm² N₂O and NO, and 0 cm³/min/cm² of NO₂ and NH₃. The bulk of the gas produced was H₂.

An expanded view of the H₂ offgas generation rate for this experiment (Figure 3-26) shows that the generation rate resulting from the use of a solution containing 2.6 M NaOH and 0.33 M NaNO₃ was greater than measured for any of the other solutions used in decladding experiments (e.g., 0.44 M NaOH/0.33 M NaNO₃, 1 M NaOH/0.75 M NaNO₃, 2 M NaOH/1.5 M NaNO₃). The H₂ offgas generation rate resulting from the use of the 2.6 M NaOH/0.33 M NaNO₃ solution to declad the mini-plate piece was comparable to the generation rate measured for Hg-catalyzed HNO₃ dissolution of Al-1100.¹⁸ The decladding was successful because the Al remained in solution rather than partially precipitating as an aluminum hydroxide species. Figure 3-27 shows 2 minutes and 27 minutes into boiling during the dissolution of Piece 3 of the mini-plate using the 2.6 M NaOH solution. There were visually more bubbles generated at the start of boiling for the 2.6 M NaOH/0.33 M NaNO₃ solution than the prior experiments and about 30 minutes into boiling the solution was dark or black from the Al spalling-off the mini-plate. After about 30 minutes of boiling, the H₂ offgas also appeared to be zero indicating the reaction had likely stopped. The mini-plate was removed after 45 minutes of boiling, rinsed, and dried (Figure 3-28). The mass of the mini-plate piece was 5.02 g which was higher than the expected mass of 4.61 g. However, as seen in the photograph of the declad mini-plate piece (Figure 3-28), the edges are thinner than the center band indicating the distribution of the Al cladding was not uniform so the estimated mass of Al would not be exactly correct. The thickness of the center band was 0.7 mm or the same thickness as measured for the unclad U-10Mo-Zr foil. The approximate Al dissolution rate was 0.02 g/min or an order of magnitude higher than measured in the earlier decladding experiments.

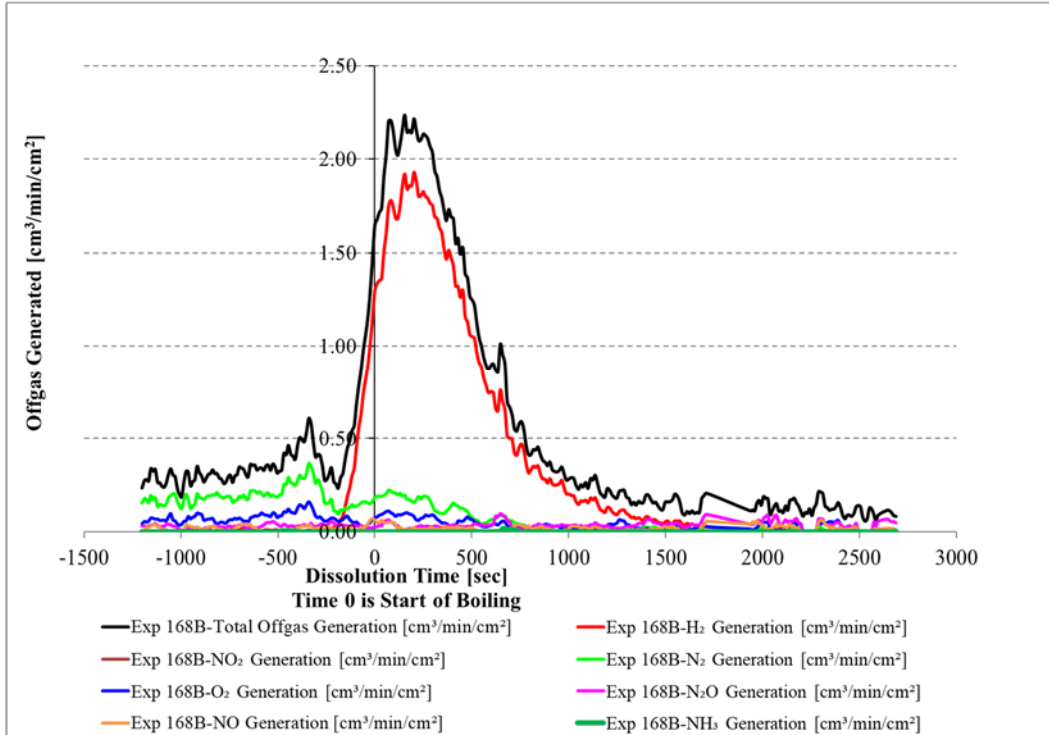


Figure 3-25. Exp 168B Offgas Generation Rates from the Decladding of Piece 3 of Mini-plate A2C116 using 2.6 M NaOH and 0.33 M NaNO₃

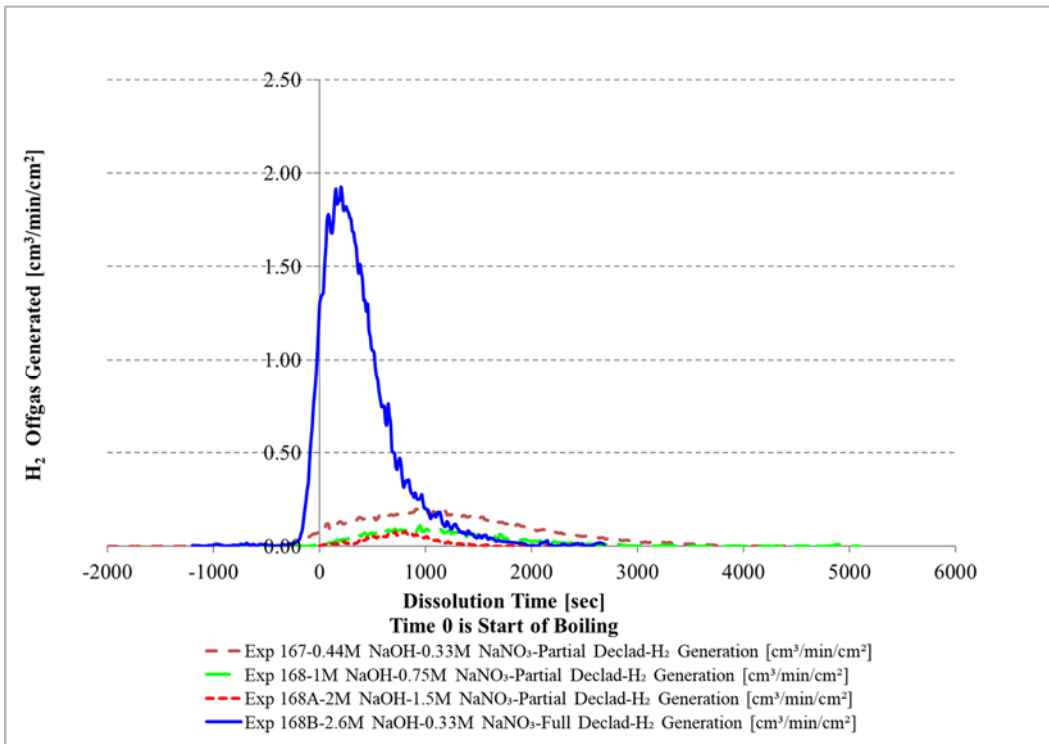


Figure 3-26. Exp 168B H₂ Generation Rate from the Decladding of Piece 3 of Mini-plate A2C116 using 2.6 M NaOH and 0.33 M NaNO₃

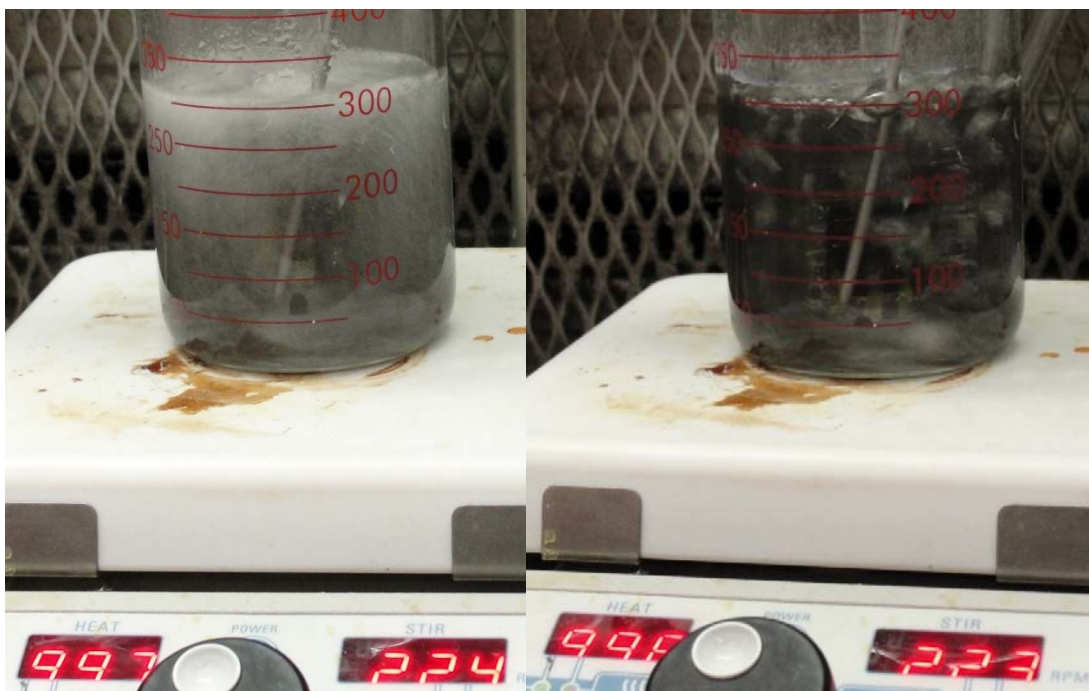


Figure 3-27. 2 min (left) and 27 min (right) into Boiling during the Decladding of Piece 3 of Mini-plate A2C116 using 2.6 M NaOH



Figure 3-28. Full Declad Piece 3 of Mini-plate A2C116

3.2.2 Flowsheet Demonstration for Declad Mini-plate

Once Piece 3 of mini-plate A2C116 was declad, a dissolution was performed (Experiment 169) targeting 20 g/L U using a 4 M HNO₃ solution containing 0.05 M fluoride to demonstrate the flowsheet developed

for the U-10Mo-Zr foil (see Section 3.1.1). The offgas generation rates during the dissolution were also measured by Raman spectroscopy (Figure 3-29). The peak total offgas rate was about $2.8 \text{ cm}^3/\text{min}/\text{cm}^2$ with approximately $2.77 \text{ cm}^3/\text{min}/\text{cm}^2$ of NO, $0.02 \text{ cm}^3/\text{min}/\text{cm}^2$ N₂, $0.01 \text{ cm}^3/\text{min}/\text{cm}^2$ O₂, $0 \text{ cm}^3/\text{min}/\text{cm}^2$ of H₂, NO₂, and N₂O. The bulk of the gas produced was NO.

An expanded view of the H₂ generation rate for Experiment 169 is plotted as a function of time in Figure 3-30. The H₂ generation rate was calculated from the measured offgas generation rate, measured H₂ concentration, and the measured surface area of the U-10Mo-Zr foil. Time zero corresponds to the start of boiling but offgas generation was measured from the point the declad foil was immersed in the solution at room temperature as it was heated to boiling. The H₂ generation rate for the dissolution of an unclad piece of U-10Mo-Zr foil (Experiment 160) is also plotted on Figure 3-30 for comparison. The H₂ generation rate was slightly higher for the unclad U-10Mo-Zr foil than for the declad foil but not significantly. This is probably a result of the formation of some oxide on the surface of the declad foil as opposed to the pristine condition of the unclad foil. The total offgas generated for the declad and unclad foil was about the same (Figure 3-31) and the majority of the offgas was NO in both experiments. Experiments 160 and 169 produced approximately the same amount of gas per time per unit area, although the declad foil produced essentially no H₂. The Raman spectrometer did not detect any significant amounts of NH₃ which is attributed to the NH₃ being reabsorbed into solution as discussed by Pierce et al.¹⁹

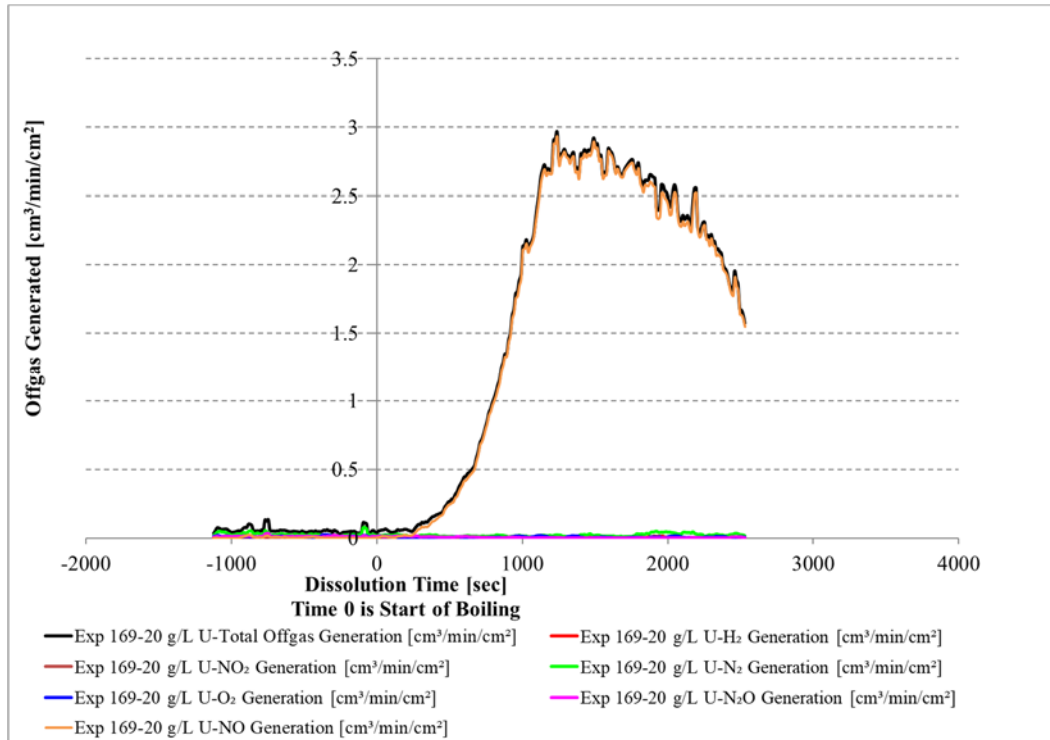


Figure 3-29. Exp 169 Offgas Generation Rates from the Dissolution of U-10Mo-Zr Foil from the Decladding of Piece 3 of Mini-plate A2C116 Targeting 20 g/L U in 4 M HNO₃ and 0.05 M Fluoride

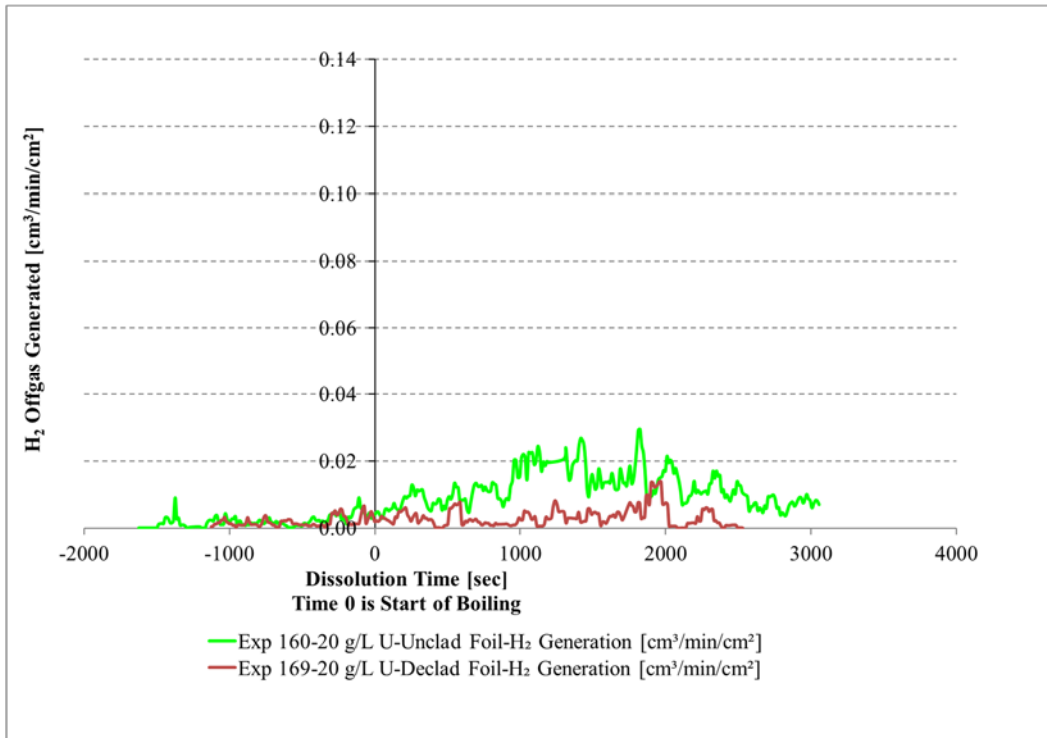


Figure 3-30. H₂ Generation Rate from the Dissolution of U-10Mo-Zr Foil from the Decladding of Piece 3 of Mini-plate A2C116 Targeting 20 g/L U in 4 M HNO₃ and 0.05M Fluoride

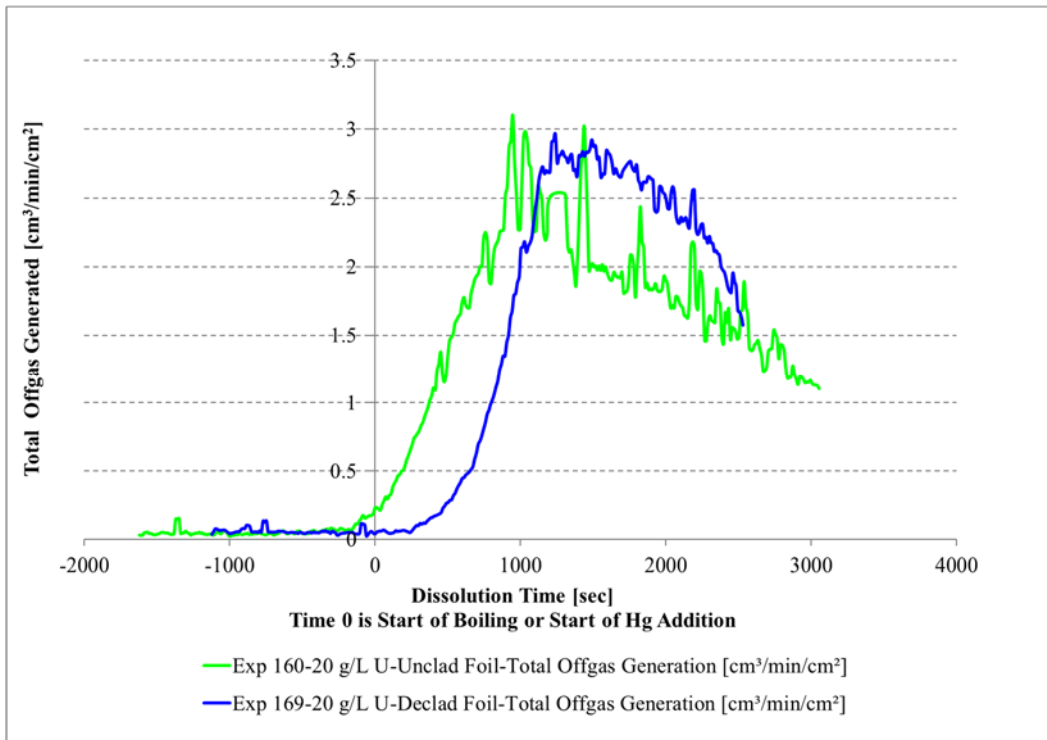


Figure 3-31. Comparison of the Total Offgas Generation Rates from the Dissolution of the Declad U-10Mo-Zr Foil in Exp 169 and the Unclad Foil Dissolved in Exp 160

4.0 Conclusions

The results for the dissolution of the U-10Mo-Zr foil are summarized in Table 4-1 where the optimum dissolution conditions are highlighted light blue. The results for the caustic decladding of the U-10Mo-Zr mini-plates are summarized in Table 4-2.

Table 4-1. Summary of Results for Dissolution of U-10Mo-Zr Foil

Exp. No.	Final U (g/L)	Objective (Evaluate)	Initial HNO ₃ (M)	Fluoride (M)	Fe(NO ₃) ₃ (M)	Precipitate	Peak H ₂ Generation (cm ³ /min/cm ²)	Dissolution Rate (g/cm ² /min)
---	---	---	(M)	(M)	(M)	---	(cm ³ /min/cm ²)	(g/cm ² /min)
156	20	U-Mo Solubility	3.00	0.05	0	Yes	---	---
157	20	U-Mo Solubility	4.00	0.05	0	No	---	---
158	20	U-Mo Solubility	5.00	0.05	0	No	---	---
159	20	Dissolution Rate	4.00	0.05	0	No	---	1.2E-02
160	20	Offgas Generation	4.00	0.05	0	No	0.02	---
161	50	U-Mo Solubility	3.00	0.1	0.50	Yes	---	---
162	50	U-Mo Solubility	4.00	0.1	0.50	No	---	---
163	50	U-Mo Solubility	5.00	0.1	0.50	No	---	---
164	50	Dissolution Rate	4.00	0.1	0.50	No	---	1.5E-02
165	50	Offgas Generation	4.00	0.1	0.50	No	0.09	---
169*	20	Offgas Generation	4.00	0.05	0	No	0.00	---

*Dissolution of U-10Mo-Zr foil after caustic decladding

Table 4-2. Summary of Results for Al Decladding of U-10Mo-Zr Mini-plates

Exp. No.	Objective (Evaluate)	Initial NaOH (M)	Initial NaNO ₃ (M)	Peak H ₂ Generation (cm ³ /min/cm ²)	Decladding Complete
---	---	(M)	(M)	(cm ³ /min/cm ²)	---
166	Offgas Generation	0.44	0.33	0.11	No
168	Offgas Generation	1.00	0.75	0.09	No
168A	Offgas Generation	2.00	1.50	0.07	No
168B	Offgas Generation	2.60	0.33	1.85	Yes

The dissolution of small pieces of U-10Mo-Zr foil at 20 g/L U with 0.05 M fluoride and 50 g/L U with 0.1 M fluoride and 0.5 M Fe using 4 and 5 M HNO₃ did not show any evidence of precipitates. However, a foil dissolution experiment at 20 g/L U using 3 M HNO₃ formed a reddish precipitate that was easily re-suspended upon shaking and eventually went into solution after 14 days. An attempt was made to characterize the solids but in moving the bottle the solids dissolved. The dissolution of a piece of foil at 50 g/L U with 0.1 M fluoride and 0.5 M Fe using 3 M HNO₃ formed a white precipitate that stuck to the glassware which was subsequently identified as a Zr-Mo compound (ZrMo₂O₅(OH)₂(H₂O)₂). There were no U products identified in the precipitate. Based on these experiments, the use of a sufficient volume of 4 M HNO₃ which results in a final acid concentration greater than approximately 3.5 M is recommended to dissolve scrap U-10Mo-Zr foil at the boiling point of the solution when targeting 20 or 50 g/L U. The fluoride concentration should be adjusted to establish a 4:1 mole ratio of fluoride to Zr and 0.5 M Fe (as Fe(NO₃)₃) added to the solution for a final target U concentration of 50 g/L to prevent U-Mo precipitates.

The dissolution rates of the U-10Mo-Zr foil in 4 M HNO₃ for both 20 g/L U (0.05 M fluoride) and 50 g/L U (0.1 M fluoride and 0.5 M Fe) were measured at the boiling point of the solutions. The dissolution rates were in the range of 1.2E-02 to 1.5E-02 g/cm²/min for both flowsheets. In each dissolution experiment, there was an initial slower dissolution rate of 4E-03 to 6E-03 g/cm²/min which was attributed to the

dissolution of the Zr diffusion barrier on the exterior of the U-10Mo foil. The measured rates can be used to estimate dissolution times for scrap U-10Mo-Zr foil generated during the fabrication of HPRR fuel.

The H₂ generation rates during the dissolution of U-10Mo-Zr foil at 20 g/L U (0.05 M fluoride) and 50 g/L (0.1 M fluoride and 0.5 M Fe) were measured using Raman spectroscopy. The peak H₂ generation rates were 0.02 cm³/min/cm² and 0.09 cm³/min/cm² for 20 g/L U and 50 g/L U, respectively. The H₂ generation rates increase once the boiling point of the solution was reached. Since the acid concentrations were the same in both experiments, the higher H₂ generation rate for the 50 g/L U dissolution was attributed to the higher fluoride concentration (about twice that of the 20 g/L U dissolution). The H₂ generation rates are small compared to the H₂ generation rate during the Hg-catalyzed dissolution of Al alloys (e.g., Al-1100) in HNO₃ which normally peak around 2 cm³/min/cm² and should be manageable by supplying an air purge to the dissolver.

The caustic removal of Al cladding from U-10Mo-Zr mini-plates with a flowsheet used in the SRS F-Canyon facility to remove Al cladding from natural and depleted U targets used for Pu production was not successful. The NaOH concentration was not sufficient to prevent precipitation of aluminum hydroxide-containing compounds. Small scale decladding experiments demonstrated that a solution containing 9.37 moles of NaOH and 1.27 moles of NaNO₃ per mole of Al was sufficient to declad the mini-plates and prevent the precipitation of Al in the basic solution. These ratios have not been fully optimized and it may be possible to use a lower molar ratio of NaOH to Al and achieve the same decladding results without forming precipitates. The H₂ offgas generation rate for decladding Al using the higher molar ratio of NaOH produced a peak H₂ offgas rate of about 2 cm³/min/cm² or a rate comparable to the Hg-catalyzed dissolution of Al-1100 in HNO₃. The H₂ offgas generation rate would be manageable with an appropriate air purge to the dissolver.

The dissolution of a piece of a U-10Mo-Zr mini-plate following cladding removal was demonstrated using the flowsheet developed for unclad foil. Dissolution of the declad foil at 20 g/L U (0.05 M fluoride) in 4 M HNO₃ was successfully performed. The total offgas generation per unit surface area was similar to the unclad U-10Mo-Zr foil. During both dissolutions, the primary offgases were NO and NO₂ (approximately 90-99% of total offgas) with the balance being H₂. The H₂ generation rate for the declad foil was noticeably lower than the unclad foil. This is likely due to the formation of some oxide on the surface of the declad foil as opposed to the pristine condition of the unclad foil. Even if the declad foil had the same H₂ generation rate as the unclad foil, the H₂ generation rate is relatively low and is manageable with an air purge.

5.0 Future Work

Future work will include the development of dissolution flowsheets for scrap streams generated during the casting of the U-10Mo alloy. Skull oxide and metal samples from the Y-12 casting process will be shipped to SRNL for use in this work.

Although not required, if lower terminal HNO₃ concentrations were desired following dissolution of U-10Mo-Zr foil, additional experiments and solubility modelling would be necessary to understand the solution conditions necessary to form the reddish precipitate observed at 20 g/L U and the Zr-Mo precipitate observed at 50 g/L U when 3 M HNO₃ was used as the dissolving solution. The ratios of NaOH and NaNO₃ to Al used to declad the U-10Mo-Zr foil were not fully optimized and it may be possible to use lower ratios to achieve the same results without precipitation. Additional experiments and solubility modelling would be necessary to understand the solution equilibria and prevent the precipitation of Al.

6.0 References

1. K. A. Dunn, G. L. Fredrickson, T. S. Rudisill, G. F. Vandegrift, and M. A. Williamson, *Uranium Recovery from Scrap Generated During Fabrication of USHPRR Fuel*, SRNL-TR-2017-00306, Savannah River National Laboratory, Aiken, SC (September 2017).
2. D. C. Stepinski, L. Maggos, J. Swanson, J. Stevens, and G. F. Vandegrift, *Scrap Recovery Operations in the Fuel Fabrication Capacity*, RERTR 2008 – 30th International Meeting on Reduced Enrichment for Research and Test Reactors, Washington, DC (October 2008).
3. D. C. Stepinski, J. Swanson, J. Stevens, and G. F. Vandegrift, *Dissolution of U-Mo-Alloy Scrap from Fuel Fabrication*, ANL/CSE-13/37, Argonne National Laboratory, Argonne, IL (2008).
4. J. Jerden, J. Fortner, and D. Stepinski, *Dissolution of Zirconium-Bonded Monolithic, Uranium-Molybdenum Fuel for Uranium Recovery*, ANL/SCE-13/30, Argonne National Laboratory, Argonne, IL (May 2009).
5. A. J. Youker, L. E. Maggos, D. C. Stepinski, A. J. Bakel, and G. F. Vandegrift, *Fuel Fabrication Capability (FFC) Scrap Recycle Report*, ANL/CSE-13/6, Argonne National Laboratory, Argonne, IL (September 2009).
6. A. J. Youker, D. C. Stepinski, L. E. Maggos, A. J. Bakel, and G. F. Vandegrift, *Aqueous processing of U-10Mo Scrap for high performance research reactor fuel*, J Nucl Mater, 427, p. 185-192 (2012).
7. A. J. Ziegler, L. E. Maggos, D. C. Stepinski, A. J. Bakel, and G. G. Vandegrift, *Scrap Recovery for Fabrication of U-10Mo fuel for High Performance Research Reactors*, RERTR – 31st International Meeting on Reduced Enrichment for Research and Test Reactors, Beijing, China (November 2009).
8. P. Faugeras, C. Lheureux, and P. Leroy, *Etude De Solubilite Du Molybdene en Miliieu Nitrique*, CEA Report No.1823, Nuclear Study Center, Seclay, France (1961).
9. W. W. Schulz and E. M. Duke, *Reprocessing of Low-Enrichment Uranium-Molybdenum Alloy Fuels*, HW-62086, General Electric Company, Richland, WA (September 1959).
10. T. J. Colven, C. W. Cline, and A. E. Wible, *Processing of Irradiated Natural Uranium at Savannah River*, DP-500, E. I. du Pont de Nemours & Co., Aiken, SC (August 1960).
11. S. L. Garrison, M. C. Lind, N. M. Askew, and G. G. Kessinger, *Uranium-Zirconium Dissolution in Nitric Acid*, SRNL-L5200-2009-00005, Savannah River National Laboratory, Aiken, SC (March 5, 2009).
12. J. L. Swanson, *An Estimation of the Explosion Hazard During Reprocessing of Metallic Uranium Fuel Elements Metallurgically Bonded to Zircaloy Cladding*, HW-62109, Hanford Atomic Products Operation, Richland, WA (September 1959).
13. R. P. Larsen, R. S. Shor, H. M. Feder, and D. S. Flikkema, *A Study of the Explosive Properties of Uranium-Zirconium Alloys*, ANL-5135, Argonne National Laboratory, Argonne, IL (July 1954).
14. W. G. Moffatt, *The Handbook of Binary Phase Diagrams*, Volume 5, Genium Publishing Corporation, Schenectady, NY (1995 revision).
15. Baseline Change Request, *Scrap Recovery Solutions and Technology Maturation Options*, SRNL-L6000-2018-00017, Savannah River National Laboratory, Aiken, SC (April 4, 2018).
16. T. S. Rudisill and W. E. Daniel, *Task Technical and Quality Assurance Plan for the Development of Dissolution Flowsheets for Scrap Generated during Fabrication of U-Mo High Performance Research Reactor Fuel*, SRNL-RP-2018-01126, Savannah River National Laboratory, Aiken, SC (March 2019).
17. W. E. Daniel, T. S. Rudisill, P. M. Almond, and P. E. O'Rourke, *Dissolution of Low Enriched Uranium from the Experimental Breeder Reactor-II Fuel Stored at the Idaho National Laboratory*, SRNL-STI-2017-00263, Savannah River National Laboratory, Aiken, SC (June 2017).
18. W. E. Daniel, T. S. Rudisill, and P. E. O'Rourke, *Dissolution of Material Test Reactor Fuel in an H-Canyon Dissolver*, SRNL-STI-2016-00725, Revision 1, Savannah River National Laboratory, Aiken, SC (May 2018).
19. R. A. Pierce and N. S. Karay, *Aluminum Metal Dissolution for Mark-18A Target Processing*, SRNL-TR-2016-00342, Revision 0, Savannah River National Laboratory, Aiken, SC (December 2016).

Distribution:

timothy.brown@srnl.doe.gov
alex.cozzi@srnl.doe.gov
david.crowley@srnl.doe.gov
c.diprete@srnl.doe.gov
a.fellinger@srnl.doe.gov
samuel.fink@srnl.doe.gov
nancy.halverson@srnl.doe.gov
erich.hansen@srnl.doe.gov
connie.herman@srnl.doe.gov
joseph.manna@srnl.doe.gov
john.mayer@srnl.doe.gov
daniel.mccabe@srnl.doe.gov
gregg.morgan@srnl.doe.gov
frank.pennebaker@srnl.doe.gov
amy.ramsey@srnl.doe.gov
william.ramsey@srnl.doe.gov
michael.stone@srnl.doe.gov
boyd.wiedenman@srnl.doe.gov
bill.wilmarth@srnl.doe.gov
charles.nash@srnl.doe.gov
kerry.dunn@srnl.doe.gov
greg.chandler@srnl.doe.gov
alexcia.delley@srs.gov
lisa.ward@srnl.doe.gov
gene.daniel@srnl.doe.gov
tracy.rudisill@srnl.doe.gov
patrick.o'rourke@srnl.doe.gov
Records Administration (EDWS)